

Specific features of heavy quark production: Local parton-hadron duality approach to heavy particle spectra

Yu. L. Dokshitzer*

Theoretical Physics Division, CERN, CH-1211, Geneva 23, Switzerland

V. A. Khoze*

Centre for Particle Theory, University of Durham, Durham DH1 3LE, United Kingdom

S. I. Troyan

Institute for Nuclear Physics, St. Petersburg, Gatchina 188350, Russia

(Received 13 June 1995)

A perturbative QCD formula for inclusive energy spectra of heavy quarks from heavy quark initiated jets, which takes into account collinear and/or soft logarithms in all orders, the exact first order result, and two-loop effects is applied to distributions of heavy flavored hadrons in the framework of the local parton-hadron duality concept.

PACS number(s): 13.65.+i, 12.38.Bx, 13.87.-a

I. INTRODUCTION

Heavy flavor physics is now extensively studied experimentally at both e^+e^- and hadronic colliders. Experiments at Z^0 have led to the availability of new data on the profiles of jets initiated by heavy quarks [1,2]. Further progress is expected from the measurements at the CERN e^+e^- collider LEP 2 and, especially, at a future linear e^+e^- collider. The principal physics issues of these studies are related not only to testing the fundamental aspects of QCD, but also to their large potential importance for measurements of heavy particle properties: lifetimes, spatial oscillations of flavor, searching for CP -violating effects in their decays, etc. Properties of b -initiated jets are of primary importance for analysis of the final state structure in $t\bar{t}$ production processes. A detailed knowledge of the b -jet profile is also essential for the Higgs boson search strategy.

The physics of heavy quarks has always been considered as one of the best testing grounds for QCD. Despite this, not many attempts to derive self-consistent perturbative theory (PT) results for the profiles of heavy quark jets have appeared so far. This paper is aimed at a condensed presentation of the part of the results of the long-term Leningrad-St. Petersburg QCD group project¹ that concerns PT analysis of the inclusive energy spectra of heavy quarks.

The selection of this subject is motivated by the following topical questions: (i) To what extent can the heavy quark distribution be treated as a purely perturbative

(infrared safe) quantity? (ii) Can we describe the gross features of jets initiated by heavy quarks without invoking phenomenological fragmentation schemes? (iii) What kind of information can be extracted from the measurements of heavy quark energy spectra and, in particular, from the scaling violation effects?

There are two ingredients of the standard renormalization group (RG) approach to the description of the energy spectra of heavy flavored hadrons H_Q . Here one starts from a phenomenological fragmentation function for the

$$Q(x) \rightarrow H_Q(x_H) \quad (1.1)$$

transition and then traces its evolution with the annihilation energy W by means of PT QCD. Realistic fragmentation functions [9] exhibit a parton-model-motivated maximum at (hereafter M is the heavy quark mass)

$$1 - \frac{x_H}{x} \sim \frac{\text{const}}{M}$$

Taking gluon radiation at the PT stage of evolution into account would then induce scaling violations that soften the hadron spectrum by broadening (and damping) the original maximum and shifting its position to larger values of $1 - x_H$ with W increasing.

This approach has been successfully tried by Mele and Nason [10], who have studied the effects of multiple soft gluon radiation and have been looking for realistic fragmentation functions to describe the present day situation with heavy particle spectra and to make reliable predictions for the future. Being formally well justified, such an approach, however, basically disregards the effects that the finite quark mass produces on the accompanying QCD bremsstrahlung pattern, since the W evolution by itself is insensitive to M (save the power-suppressed M^2/W^2 corrections).

At the same time, as far as one may consider M a sufficiently large momentum scale, it is tempting to carry

*On leave of absence from the Institute for Nuclear Physics, St. Petersburg, Gatchina 188350, Russia.

¹For some basic references, see [3-8].

out a program of deriving the predictions that would keep under PT control, as much as possible, the dependence of H_Q distributions on the quark mass.

In Sec. II we present and discuss the PT formula for inclusive quark spectra $D(x; W, M)$ that in the QED case would give an unambiguous all-order-improved *absolute* prediction for the inclusive energy distribution of muons produced in

$$e^+e^- \rightarrow \mu^\pm(x)\mu^\mp + \dots \quad (1.2)$$

Given an explicit dependence on m_μ , one may theoretically compare, say, the μ and τ spectra, a goal that, generally speaking, cannot be achieved within the standard "evolutionary" framework.

In Sec. III the topical questions listed above are addressed. We discuss the problem of "infrared instability" of the PT quark spectra and suggest a solution of this formal difficulty based upon the notion of an "infrared regular" effective coupling. Having regularized the PT expression in this way, we observe that the gluon bremsstrahlung effects (Sudakov suppression of the quasielastic kinematics $x \rightarrow 1$) lead to particle spectra that have a similar shape to the non-PT fragmentation function.

An emphasis of the role of PT dynamics has been successfully tested in studies of light hadron distributions in QCD jets. Prompted by the success of the MLLA-LPHD approach [11], we consider an option of describing the gross features of heavy-quark-initiated jets entirely by means of PT QCD, without invoking any fragmentation hypothesis.

The LPHD philosophy would encourage us to continue the PT description of an inclusive quantity down to small momentum scales and with the hope that such an extrapolation of the quark-gluon language would be dual to the sum over all possible hadronic excitations. For the problem under consideration, such an approach could describe the energy fraction distribution averaged over heavy-flavored hadron states, the mixture that naturally appears, e.g., in the study of inclusive hard leptons.

In Sec. IV, we report results on the comparison of the PT predictions with the measured c and b energy losses at different annihilation energies. Fitting the rate of scaling violation in $\langle x \rangle(W)$ results in the QCD scale parameter Λ that, after being translated into the popular modified minimal subtraction ($\overline{\text{MS}}$) scheme, agrees with the values extracted from other studies. On the other hand, the *absolute* values of $\langle x_{c,b} \rangle$ at a given energy are most sensitive to the behavior of the radiation intensity, say, below 1–2 GeV.

Limited experimental information does not at present allow us to disentangle various possible shapes of α_s^{eff} near the origin. At the same time, a quite substantial difference between $\langle x_c \rangle$ and $\langle x_b \rangle$ fits nicely into the PT-controlled mass dependence, provided the characteristic integral of the effective coupling over the "confinement" region assumes a fixed value:

$$\int_0^2 \frac{\text{GeV}}{dk} \frac{\alpha_s^{\text{eff}}(k)}{\pi} \approx 0.38 \text{ GeV}$$

(with k the linear momentum variable). Given this value, one may predict the differential c and b energy distributions at arbitrary W , predictions which prove to be unaffected in practice by our ignorance of the detailed behavior of α_s^{eff} in the small momentum region.

In Sec V the results of the study are discussed and conclusions are drawn.

A detailed derivation of the master formula for the inclusive heavy quark energy spectrum is given in the Appendixes. In Appendix A the problem of running coupling in the perturbative radiator is dealt with. Appendix B is devoted to second loop effects in the anomalous dimension.

II. PERTURBATIVE ENERGY SPECTRUM OF LEADING QUARKS

We denote the c.m. system (c.m.s.) annihilation energy by W , and $M \equiv mW$ is the quark mass. Here we describe perturbative QCD results for the inclusive energy spectrum of heavy quarks, $D(x; W, M)$, $x \equiv 2E_Q/W$, produced in $e^+e^- \rightarrow Q(x) + \bar{Q} + \text{light partons}$.

This function has the following properties: It embodies the exact first order results [12] $D^{(1)} = \alpha_s f(x; m)$, and as a consequence, it has the correct threshold behavior at $1 - 2m \ll 1$; in the relativistic limit $m \ll 1$, it accounts for all significant logarithmically enhanced contributions in high orders, including (1) running coupling effects, (2) the two-loop anomalous dimension, and (3) the proper coefficient function with exponential Sudakov-type logarithms, which are essential in the quasielastic kinematics, $(1-x) \ll 1$; it takes into full account the controllable dependence on the heavy quark mass that makes possible a comparison between the spectra of b and (directly produced) c quarks.

By "threshold behavior" we mean here the kinematical region of nonrelativistic quarks, $|W - 2M| \sim M$, in which gluon bremsstrahlung acquires additional dipole suppression. At the same time we will not account for the Coulomb effects that would essentially modify the production cross section near the actual threshold, $W - 2M \ll M$ [13].

We are mainly interested in the "leading" energy region of x of order of (or close to) unity. For this reason we disregard in what follows potentially copious production of $Q\bar{Q}$ pairs via secondary gluon splitting,² i.e., *singlet* sea contribution, as well as the specific $Q \rightarrow Q + Q\bar{Q}$ transition that appears in the *nonsinglet* anomalous dimension beyond the first loop (for a review see [14] and references therein).

Therefore the quark distribution we define below will satisfy the sum rule

$$\int_{2m}^1 dx D(x; W, M) = 1. \quad (2.1)$$

²Apart from the integral effect of the unregistered pairs embodied into the running coupling; see below.

The accuracy of the PT prediction described in this paper is

$$D(x; W, M)[1 + O(\alpha_s^2)] . \quad (2.2)$$

This expansion is *uniform* in x ; that is, the α_s^2 correction does not blow up (neither as a power nor logarithmically) when $(1-x) \rightarrow 0$.

A. Definition of the leading quark distribution

The inclusive cross section for single-particle production in e^+e^- annihilation is conveniently written in terms of structure functions as, e.g., [14]

$$\sigma_0^{-1} \frac{d\sigma}{dx} = 3\mathcal{F}_L^+(x) + \mathcal{F}_2^+(x) = \mathcal{F}_L^+(x) + \mathcal{F}_T^+(x) , \quad (2.3)$$

with σ_0 the standard Born cross section factor.

We define the normalized inclusive energy spectrum as

$$D(x; W, M) = \sigma_{\text{tot}}^{-1} \frac{d\sigma}{dx} \equiv \int_{\Gamma} \frac{dj}{2\pi i} x^{-j} D_j(W, M) , \quad (2.4)$$

where the contour Γ runs parallel to the imaginary axis in the complex moment j plane.

Aiming at an *exact* account of the first order QCD effects, we include in σ_{tot} the first α_s correction to the annihilation cross section, which in the case of relativistic quarks reads

$$\sigma_{\text{tot}} = \sigma_0 [1 + \frac{3}{2} C_F a + O(a^2)] , \quad a = a(W^2) \equiv \frac{\alpha_s(W)}{2\pi} , \quad C_F = \frac{N_c^2 - 1}{2N_c} = \frac{4}{3} .$$

With this definition, the structure functions \mathcal{F} in the moment representation become

$$\begin{aligned} \mathcal{F}_\alpha(j) &= c_\alpha(j) (1 - \frac{3}{2} C_F a [j^{-1} - 1]) D_j [1 + O(a^2)] , \\ c_L(j) &= C_F a j^{-1} , \quad c_T(j) = 1 + \frac{1}{2} C_F a j^{-1} , \quad c_2(j) = 1 - \frac{3}{2} C_F a j^{-1} . \end{aligned} \quad (2.5)$$

B. Radiator

The integrand of (2.4) may be written in the exponential form as

$$\ln D_j = \int_{2m}^1 dx [x^{j-1} - 1] \frac{dw(x; W, M)}{dx} , \quad (2.6)$$

where the "radiator" dw/dx originates from the improved first order gluon emission probability, in which finite mass and running coupling effects have been included.³ The corresponding expression reads

$$C_F^{-1} \nu \frac{dw}{dx} = \int_{\kappa^2}^{Q^2} \frac{dt}{t} \left\{ a(t) \left[\frac{2(x-2m^2)}{1-x} + \zeta^{-1}(1-x) \right] - a'(t)(1-x) + a^2(t) \Delta^{(2)}(x) \right\} \quad (2.7a)$$

$$+ \beta(x) \left\{ -\frac{2x}{1-x} [a(Q^2) + a(\kappa^2)] + \zeta^{-1} \frac{x(x-2m^2)}{2(1-x)} \left(\frac{1-x}{1-x+m^2} \right)^2 a(Q^2) \right\} . \quad (2.7b)$$

Here the two characteristic momentum scales have been introduced:

$$Q^2 \equiv Q^2(x) = W^2 \frac{(1-x)^2}{1-x+m^2} z_0 , \quad (2.8)$$

$$\kappa^2 \equiv \kappa^2(x) = M^2 \frac{(1-x)^2}{z_0} ,$$

with

$$z_0 \equiv \frac{1}{2} (x - 2m^2 + \sqrt{x^2 - 4m^2}) = x + O(m^2) .$$

³Detailed derivation of the radiator is presented in Appendix A; see also [7].

The following notation was also used:

$$m \equiv \frac{M}{W} \leq \frac{1}{2}, \quad v \equiv \sqrt{1-4m^2}, \quad \beta(x) \equiv \sqrt{1-4m^2/x^2}, \quad 0 \leq \beta \leq v, \quad \zeta = 1 + 2m^2,$$

$$a'(k^2) = \frac{d}{d \ln k^2} a(k^2), \quad a(k^2) \equiv \frac{\alpha_s(k)}{2\pi}. \quad (2.9)$$

The radiator (2.7) vanishes at

$$x = x_{\min} \equiv 2m; \quad \left(\beta(x_{\min}) = 0, \quad Q^2 = WM \frac{(1-2m)^2}{1-m} = \kappa^2 \right),$$

thus justifying the lower kinematical limit in Eq. (2.6).

1. Relativistic approximation

In the relativistic approximation, $m \ll 1$, we set $v = \beta = \zeta = 1$ to get a simplified expression

$$C_F^{-1} \frac{dw}{dx} = \int_{\kappa^2}^{Q^2} \frac{dt}{t} \{ a(t)P(x) - a'(t)(1-x) + a^2(t)\Delta^{(2)}(x) \} + a(Q^2) \left\{ \frac{-2x}{1-x} + \frac{x^2}{2(1-x)} \right\} + a(\kappa^2) \left\{ \frac{-2x}{1-x} \right\}, \quad (2.10a)$$

$$Q^2 = W^2 x(1-x), \quad \kappa^2 = M^2(1-x)^2/x, \quad (2.10b)$$

where

$$P(x) = \frac{1+x^2}{1-x}. \quad (2.11)$$

The integration variable t determines the physical hardness scale of the running coupling and is related to the transverse momentum of the radiation.⁴ In the dominant integration region,

$$k_{\perp}^2 \ll W^2, \quad t = x \cdot k_{\perp}^2. \quad (2.12)$$

The lower limit $t \geq \kappa^2$ sets the boundary for the essential gluon emission angles:

$$t \sim E_Q \frac{2}{W} (\omega_g \Theta)^2 \geq \kappa^2 \sim M^2 \frac{\omega_g^2}{E_Q W} \\ \implies \Theta \geq M/E_Q \equiv \Theta_0.$$

This restriction manifests the “dead cone” phenomenon characteristic for bremsstrahlung off a massive particle. It is largely responsible for the differences between radiative particle production in jets produced by a light and a heavy quark (excluding the decay products of the latter); see [4–6].

C. Logarithms and their exponentiation

Singularities of the radiator (2.7) at $x = 1$, when driven through the inverse Mellin transform (2.4), (2.6), give rise to $\ln(1-x)$ terms. Bearing this in mind, one may represent the term-by-term structure of the radiator by the symbolic expression

$$(2.7a) \implies a(CS + S^2) + aC + a^2C \\ + [a^2C + \underline{a^2(CS + S^2)}], \quad (2.13a)$$

$$(2.7b) \implies aS + aS + aS, \quad (2.13b)$$

where $C = \ln W/M$ and $S = \ln 1/(1-x)$ represent large logarithms that usually reflect enhancements due to quasicollinear and soft gluon radiation, respectively. As we shall see shortly, under the “physical” definition of the QCD coupling the last second order term in (2.13a) is free from the double-logarithmic contribution (the underlined piece) so that the “convergence” of the PT expansion (2.13) is improved.

Exponentiation of collinear logarithms follows from the general factorization theorem.⁵ Arguments in favor of

⁴For the spacelike evolution, a similar relation holds [15] with x^{-1} substituted for x in (2.12).

⁵This applies to C -contaminated terms of (2.13a) as well as to the last contribution in (2.13b), which actually is due to hard gluons collinear to the \bar{Q} momentum (the “backward jet” correction [7]).

exponentiation of $aS^2 + aS$ contributions according to (2.6) have been given in [7], motivated by the factorization property of soft bremsstrahlung. Exponentiation of nonlogarithmic $O(a)$ corrections, corresponding to the terms in the nonintegral part of the radiator (2.7a) that are *regular at* $(1-x) \rightarrow 0$, is questionable (indeed wrong) and unnecessary within the accuracy adopted [see (2.2)]. Keeping such terms in the exponent is a matter of choice.

We do so just to simplify the result and make the normalization sum rule (2.1) automatically satisfied, $D_{j=1} \equiv 1$.

When translated into the standard language of the RG-motivated approach, the integral part of the radiator (2.10) may be said to embody the anomalous dimension together with (a part of) the correction to the hard cross section due to the x -dependent factor in the upper integration limit:

$$\int^{W^2 x(1-x)} \frac{dt}{t} a(t) P(x) \approx \int^{W^2} \frac{dt}{t} a(t) P(x) + a(W^2) P(x) \ln[x(1-x)] + O\left(\frac{a^2 \ln^2(1-x)}{1-x}\right). \quad (2.14)$$

Nonuniformity of such an expansion with respect to the potentially large logarithm, $\ln(1-x)$, explains why we preserve the exact kinematical limits in (2.7). By neglecting the last term in (2.14), one would lose control of the $a^2 S^3$ terms. Such contributions formally belong to the second order correction to the hard cross section and therefore lie beyond the reach of the two-loop RG analysis. In the meantime, such ignorance would undermine the possibility of keeping track of essential first subleading corrections, $a^n \log^{2n-1}$, at the level of running coupling effects in the quark form factor (Sudakov suppression).

Let us stress that Eqs. (2.6), (2.7) solve the problem of all-order resummation of soft radiation effects both in the *hard cross section*⁶ and in the *coefficient function*, which is at low-momentum scales $\kappa^2 \propto M^2$. In particular, the term in (2.7b) proportional to $a(\kappa^2)$ (which is W independent and therefore gets lost in the standard evolution approach) accounts for the *exponentiated* contri-

bution from soft gluons at small emission angles $\Theta < \Theta_0$, $k_{\perp}^2 \ll M^2$, the dead cone subtraction effect. Notice that the similar term proportional to $a(Q^2)$ (which does belong to the hard cross section corrections) is due to the dead cone subtraction in the backward jet.

D. Second loop effects

The preliminary result of [7] is improved by taking into full account effects of the two-loop anomalous dimension embodied in the a' and $\Delta^{(2)}$ of (2.7a). We prefer to treat these two terms separately, as the former naturally emerges in the dispersion relation approach to definition of the running coupling [17]. It shows that beyond the first loop the "soft" and "hard" parts of the Gribov-Lipatov-Altarelli-Parisi (GLAP) splitting function (2.11) in the anomalous dimension actually acquire different physical interaction strengths [15]:

$$\gamma^{(1)} = a \frac{1+x^2}{1-x} \implies \gamma^{(2)} = a \frac{2x}{1-x} + [a - a'](1-x).$$

The actual expression for Δ depends on the renormalization scheme chosen for the one-loop coupling. It may be fixed, e.g., by matching with the known two-loop $\overline{\text{MS}}$ result for the nonsinglet fragmentation function. To this end one has to consider the W -dependent part of the relativistic radiator (2.10),

$$C_F^{-1} \frac{dw}{dx} = \int^{W^2 x(1-x)} \frac{dt}{t} \{ a_{\overline{\text{MS}}}(t) P(x) - a'(t)(1-x) + a^2(t) \Delta_{\overline{\text{MS}}}^{(2)}(x) \} + a(W^2) \left\{ \frac{-2x}{1-x} + \frac{x^2}{2(1-x)} \right\} + \text{const} + O(a^2(W^2)), \quad (2.15)$$

and, with account of (2.5) relating D to the structure functions, compare the scaling violation rate according to (2.6), (2.15) with that computed in [18-20].

By doing so (see Appendix B) one arrives at ($C_A = N_c = 3$, $T_R = \frac{1}{2}$)

$$\Delta_{\overline{\text{MS}}}^{(2)}(x) = P(x) \mathcal{K} + \tilde{\Delta}^{(2)}(x), \quad (2.16a)$$

⁶For a review of such resummation programs, see, e.g., [16] and references therein.

$$\mathcal{K} = \left[C_A \left(\frac{67}{18} - \frac{\pi^2}{6} \right) - \frac{10}{9} n_f T_R \right] = \begin{cases} 4.565 & (n_f = 3), \\ 4.010 & (n_f = 4), \\ 3.454 & (n_f = 5), \end{cases} \quad (2.16b)$$

$$\tilde{\Delta}^{(2)}(x) = C_F \mathcal{V}(x) + \mathcal{R}(x). \quad (2.16c)$$

The \mathcal{V} term is responsible for the difference between the timelike and spacelike anomalous dimensions. Explicit expressions for $\mathcal{V}(x)$ and $\mathcal{R}(x)$ are given in Appendix B.

1. Introducing the physical couplings

In the $x \rightarrow 1$ limit, $\Delta_{\overline{\text{MS}}}^{(2)}$ [Eq. (2.16)] peaks together with $P(x) \propto (1-x)^{-1}$. At the same time, $\tilde{\Delta}^{(2)}$ is less singular in this limit:

$$\mathcal{V}(x)/\Delta^{(2)}(x) \propto (1-x) \ln(1-x),$$

$$\mathcal{R}(x)/\Delta^{(2)}(x) \propto (1-x)^2.$$

As far as large quark energies are concerned, $\ln 1/(1-x) > 1$, the $\tilde{\Delta}^{(2)}$ term constitutes a small correction. Thus the major part of the two-loop effect according to (2.16) reduces to a finite renormalization of the leading term $aP(x)$. This naturally suggests absorbing the correction by introducing the “physical” effective coupling according to

$$\begin{aligned} a_{\overline{\text{MS}}} P(x) + a^2 \Delta_{\overline{\text{MS}}}^{(2)}(x) \\ = a_{\text{eff}} P(x) + a^2 \tilde{\Delta}^{(2)}(x) + O(a^3), \end{aligned} \quad (2.17a)$$

$$a_{\text{eff}} = a_{\overline{\text{MS}}}(1 + a\mathcal{K}), \quad a_{\overline{\text{MS}}} \approx a_{\text{eff}}(1 - a_{\text{eff}}\mathcal{K}). \quad (2.17b)$$

Equation (2.17b) relates the scale parameters Λ of the two schemes. This relation within two-loop accuracy reads

$$\begin{aligned} \ln \Lambda_{\text{eff}} &= \ln \Lambda_{\overline{\text{MS}}} + \frac{\mathcal{K}}{\beta} \\ &= \ln \Lambda_{\overline{\text{MS}}} + \frac{(\frac{67}{18} - \frac{\pi^2}{6})C_A - \frac{10}{9}n_f T_R}{\frac{11}{3}C_A - \frac{4}{3}n_f T_R}, \end{aligned} \quad (2.18)$$

$$\Lambda_{\text{eff}} = \Lambda_{\overline{\text{MS}}} \times \begin{cases} 1.66 & (n_f = 3), \\ 1.57 & (n_f = 5). \end{cases}$$

Our Λ_{eff} coincides with the Λ_{MC} introduced by Catani, Marchesini, and Webber in [21].

2. Quark thresholds in the running coupling

One additional comment is in order concerning the essence of α_s^{eff} . In spite of the formal equivalence of

the two representations (2.17a), the former one is physically preferable since $\tilde{\Delta}^{(2)}(x)$ is free from an ill-defined quantity n_f representing the number of “active” quark flavors. The t integration in (2.7) runs over a broad region that is sliced by the finite quark mass scales. Naturally, one has to increment n_f when passing such a scale, e.g., $n_f = 3 \rightarrow n_f = 4$, when going through $t \approx 1.5$ GeV. $\Lambda_{\overline{\text{MS}}}$ has to be redefined by adjusting to a new β -function value, and $\Delta_{\overline{\text{MS}}}$ should be changed accordingly. The problem appears to be entirely technical, however, and reflects a deficiency of the $\overline{\text{MS}}$ prescription as one of the schemes based upon the dimensional regularization technique that eventually treats fermions as massless particles: The discontinuous behavior of Λ and Δ gets compensated in the physical combination (2.17a) that emerges in the full two-loop anomalous dimension. It is worthwhile to notice that our convention [n_f -independent $\tilde{\Delta}^{(2)}(x)$, the scale parameter Λ defined by (2.18)] is in accordance with the Brodsky-Lepage-Mackenzie (BLM) prescription [22] for optimizing the choice of “physical coupling.”

For argument’s sake, one may once again invoke the QED example (1.2). In this context, an application of the $\overline{\text{MS}}$ scheme would reveal the same problem with the lepton thresholds (e, μ, τ , etc.), while a_{eff} would be nothing but the *physical* running QED coupling, the one given by the Euclidean photon renormalization function $Z_3(t)$ that is unambiguously linked by the dispersion relation to fermion pair production (with the finite fermion mass effects fully included).

The improved one-loop expression for a_{eff} accounting for finite quark mass effects reads (for a detailed discussion, see [15])

$$\begin{aligned} a_{\text{eff}}^{-1}(Q^2) &= \beta_l \ln \frac{Q}{\mu} - \frac{2T_R}{3} \sum_i \Pi \left(1 + \frac{4M_i^2}{Q^2} \right) \\ &\quad + a_{\text{eff}}^{-1}(\mu^2) \quad (\mu \ll M_i), \end{aligned} \quad (2.19a)$$

$$\Pi \approx \begin{cases} \ln(Q^2/M_i^2) - \frac{5}{3}, & Q \gg M_i, \\ 2Q^2/5M_i^2, & Q \ll M_i, \end{cases} \quad (2.19b)$$

where β_l accounts for gluon and massless quark contributions ($\beta_l = b_{[n_f=3]} = 9$) and Π is the standard fermion loop polarization operator known from the mid-1950s [see below Eq. (3.24)]. According to (2.19b), heavy flavors *decouple* at low momentum scales (as they ought to). In the “ultraviolet” regime, Π acquires a constant subtraction from the leading logarithmic behavior, which term, if treated as the two-loop correction, explains the n_f -

dependent piece of the \mathcal{K} factor (2.16b) that enters the relation (2.17b) between the physical and $\overline{\text{MS}}$ couplings: $-\frac{10}{9}T_R = \frac{4}{3}T_R(-\frac{5}{6})$.

3. $\tilde{\Delta}^{(2)}$ is practically negligible

As an estimate of the magnitude of the $\tilde{\Delta}^{(2)}$ correction, we present its contribution to the second moment $j = 2$ that describes quark energy losses:

$$\begin{aligned} C_F \{ a_{\overline{\text{MS}}} P_j (1 + a\mathcal{K}) + a^2 \tilde{\Delta}_j^{(2)} \} \\ = C_F P_j \{ a_{\text{eff}} + a^2 \delta_j \} + O(a^3), \\ \delta_2 = \left[\frac{21}{36} + \left(\frac{85}{36} - \frac{\pi^2}{3} \right) \right] C_F + \frac{31}{36} (C_A - 2C_F) \\ = -0.1735. \quad (2.20) \end{aligned}$$

Being numerically very small already for $j = 2$, the relative correction δ_j continues to fall as j^{-1} with j increasing. Therefore in practice one may use (2.7) with $\Delta^{(2)} \equiv 0$, provided the physical effective coupling (2.17b) is used.

E. Axial vs vector currents in $Q\bar{Q}$ production

The master equation (2.7) has been written for the case of $Q\bar{Q}$ production via the vector current, in which case

$$\zeta = \zeta_V \equiv \frac{\sigma_{[V]}(v)}{\sigma_{[V]}(1)} = 1 + 2m^2 = \frac{1}{2}(3 - v^2).$$

This factor tends to 1 in the relativistic limit $m \rightarrow 0$, but depends otherwise on the production channel (see Appendix A for details). It is worthwhile to note that beyond the leading twist approximation, generally speaking, there is no way to define the universal fragmentation distributions that would be independent of the production stage. The origin of such nonuniversality (that shows up at the level of $\alpha_s m^2 \ln m^2$ terms) may be traced back to the process-dependent radiation of hard gluons:⁷

$$d\sigma \propto \omega_g d\omega_g \propto (1-x) dx.$$

In practice, we have to deal with a mixture of vector and axial production currents. In the pure axial case ζ should be substituted by

$$\zeta_A \equiv \frac{\sigma_{[A]}(v)}{\sigma_{[A]}(1)} = 1 - 4m^2 = v^2.$$

⁷Both the "soft" and "semisoft" terms of the radiation spectrum, $\propto \omega_g^{-1} d\omega_g$ and $\propto 1 d\omega_g$ remain universal [23,24].

In addition, the $\zeta^{-1}(1-x)$ term in (2.7) acquires an extra mass correction factor $(1 + 2m^2)$. Both this effect and the difference between ζ_V and ζ_A are proportional to $m^2 = (M/W)^2$. We conclude that the difference between the radiation spectra in V and A channels vanishes as $(1 - v^2)$ in the relativistic case, while for nonrelativistic quarks, $v \ll 1$, the axial contribution to the cross section is relatively suppressed as $A/V \sim v^2$.

Therefore (2.4)–(2.7) may be used in practice for the realistic $V + A$ mixture, in particular, at the Z^0 peak.

III. HADRONIZATION AND INFRARED FINITE α_s

In the QCD context the non-PT phenomena inevitably enter the game. It is important to stress, however, that the strong interaction not only determines the hadronization transition (1.1), but also affects to some extent the quark evolution stage: The high order effects embodied into the *running coupling* seem to undermine the very possibility of the PT analysis.

It is often believed that the large quark mass $M \gg \Lambda$ provides a natural cutoff, which keeps the relevant space-time region compact enough to avoid the truly strong, non-PT interaction in a course of the quark evolution.

To illustrate the point we invoke a rough estimate that follows immediately from (2.6) and is valid for numerically large x values in the double-logarithmic approximation [7],

$$D(x; W, M) \propto (1-x)^{C_F \Delta \xi - 1}, \quad (3.1a)$$

with $\Delta \xi$ the characteristic evolution integral:

$$\Delta \xi = \int_{(1-x)^2 M^2}^{(1-x)W^2} \frac{dk_{\perp}^2}{k_{\perp}^2} \frac{\alpha_s(k_{\perp})}{\pi}. \quad (3.1b)$$

In the fixed coupling approximation, we would get

$$\begin{aligned} D(x) \propto (1-x)^{(C_F \alpha_s / \pi) \ln(W^2/M^2) - 1} \\ \times \exp \left\{ -\frac{C_F \alpha_s}{2\pi} \ln^2(1-x) \right\}. \quad (3.2) \end{aligned}$$

In the small coupling regime $C_F(\alpha_s/\pi) \ln \frac{W^2}{M^2} < 1$, this distribution exhibits a sharp peak at large x followed by a steep falloff in the $x \rightarrow 1$ limit due to the double logarithmic Sudakov suppression. One expects a qualitatively similar shape for the heavy hadron spectrum due to the $Q \rightarrow H_Q$ transition from parton model consideration [25] which lead to the so-called Peterson fragmentation function [9]

$$C_Q(x) = \frac{N}{x} \left[\frac{1-x}{x} + \frac{\epsilon_Q}{1-x} \right]^{-2}, \quad (3.3)$$

$$N = \frac{4\epsilon_Q^{1/2}}{\pi} [1 + O(\epsilon_Q^{1/2})].$$

This function peaks at $1 - x \approx \epsilon^{1/2} \ll 1$, leading to

$$\begin{aligned} \langle 1 - x \rangle_{\text{fragm}} &= \epsilon_Q^{1/2} \frac{2}{\pi} (\ln \epsilon_Q^{-1} - 1) [1 + O(\epsilon_Q^{1/2})] \\ &\propto \epsilon_Q^{1/2}. \end{aligned} \quad (3.4)$$

A. Peterson fragmentation function vs integrated coupling

One may single out effects of the non-PT momentum region by factorizing the D spectrum in the moment representation (2.6) into the product of the "safe" PT part and the "confinement" factor:

$$D_j = D_j[k_\perp^2 > \mu^2] D_j^{(C)}. \quad (3.5a)$$

In other words, we split the radiator into two pieces corresponding to large and small transverse momentum regions ($t \approx k_\perp^2$ for x close to 1):

$$\frac{dw}{dx} = \frac{dw}{dx}[k_\perp^2 > \mu^2] + \left\{ \frac{dw}{dx} \right\}^{(C)} [k_\perp^2 \leq \mu^2]. \quad (3.5b)$$

This formal separation becomes informative if one is allowed to choose the boundary value μ well below the quark mass scale (e.g., $\mu = 1$ GeV providing $\mu/M \ll 1$ for the b quark case). Within such a choice only x close to 1 would contribute to $w^{(C)}$. For illustrative purposes let us neglect subleading μ/M effects and retain the most singular term only to get an estimate

$$\left\{ \frac{dw}{dx} \right\}^{(C)} \approx \vartheta \left(\frac{\mu}{M} - (1-x) \right) \int_{[(1-x)M]^2}^{\mu^2} \frac{dt}{t} a(t) \frac{2C_F}{1-x} + \dots \quad (3.6a)$$

One arrives at

$$\begin{aligned} \ln D_j^{(C)} &\approx \int_0^{\mu/M} dz [(1-z)^{j-1} - 1] \int_{[zM]^2}^{\mu^2} \frac{dt}{t} a(t) \frac{2C_F}{z} \\ &= 2C_F \int_0^\mu \frac{dk}{k} \frac{\alpha_s(k)}{\pi} \int_0^k \frac{du}{u} \left[\left(1 - \frac{u}{M}\right)^{j-1} - 1 \right]. \end{aligned} \quad (3.6b)$$

It is important to stress that it is the first "confinement insensitive" factor of (3.5a) only that depends on W . Therefore the ratio of the moments

$$D_j(W, M) / D_j(W_0, M) \quad (3.7a)$$

as a function of W and the heavy quark mass is expected to be an "infrared-stable" PT prediction. Another message one receives observing the structure of the radiator (2.7) is that the ratio of the moments for *different* quarks,

$$D_j(W, M_1) / D_j(W, M_2), \quad (3.7b)$$

should tend to a W -independent confinement sensitive (*sic*) constant in the relativistic limit $W \gg M_1, M_2$.

We proceed with the estimate of the "confinement" factor (3.6b). As far as μ/M may be treated as a small parameter, for finite moments $j \sim 1$, $j\mu/M \ll 1$,

$$\ln(D_j^{(C)}) = -2C_F(j-1) \int_0^\mu \frac{dk}{M} \frac{\alpha_s(k)}{\pi} \left[1 + O\left(\frac{jk}{M}\right) \right] \approx -2C_F(j-1) \frac{\mu_\alpha}{M}, \quad (3.8)$$

with

$$\mu_\alpha \equiv \int_0^\mu dk \frac{\alpha_s(k)}{\pi}. \quad (3.9)$$

In particular, for the energy losses $j = 2$, one has

$$\ln D_2^{(C)} \equiv \ln \langle x \rangle^{(C)} = -2C_F \frac{\mu_\alpha}{M} \left[1 + O\left(\frac{\mu}{M}\right) \right], \quad \langle x \rangle^{(C)} = \exp \left\{ -2C_F \frac{\mu_\alpha}{M} \right\}. \quad (3.10)$$

If (3.8) were applicable for *all* j , the inverse Mellin transform would result in a singular distribution

$$D(x)^{(C)} = \delta(x - \langle x \rangle^{(C)}). \quad (3.11)$$

This singularity gets smeared when a proper treatment is given to the large j region. To this end one may use a simple

expression that interpolates between (3.8) and the correct logarithmic asymptote of the “confinement radiator” in (3.6):

$$\ln D_j^{(C)} \approx -2C_F \int_0^\mu \frac{dk}{k} \frac{\alpha_s(k)}{\pi} \ln \left[1 + \frac{k}{M} (j-1) \right]. \quad (3.12)$$

As a result, a distribution emerges that peaks around $x = \langle x \rangle^{(C)}$ and is rather similar in shape to (3.3). The extreme $x \rightarrow 1$ asymptote is determined by the region of parametrically large moments $\langle j \rangle \propto (1-x)^{-1} \gg M/\mu$. It is different for two regimes:

$$\alpha_s(0) > 0, \quad \ln D_j^{(C)} \sim -C_F \frac{\alpha_s(0)}{\pi} \ln^2 \left(j \frac{\mu}{M} \right) \implies D(x) \propto \frac{\exp\{-C_F[\alpha_s(0)/2\pi] \ln^2(1-x)\}}{1-x}, \quad (3.13a)$$

$$\alpha_s(0) = 0, \quad \ln D_j^{(C)} \sim -2C_F \Xi_0 \ln \left(j \frac{\mu}{M} \right) \implies D(x) \propto (1-x)^{-2C_F \Xi_0 - 1}, \quad (3.13b)$$

where, in the latter case,

$$\Xi_0 \equiv \int_0^\mu \frac{dk}{k} \frac{\alpha_s(k)}{\pi} < \infty. \quad (3.14)$$

Reproducing the concrete behavior of the Peterson function (3.3) in the large x limit, $C(x) \sim (1-x)^2$, would require $\Xi_0 = \frac{9}{8}$ in the second regime (3.13b). We conclude that the particle distribution originating from (3.6) is capable of reproducing the gross features of the popular Peterson fragmentation function (provided, naturally, that the notion of the infrared regular effective coupling is implanted in the PT-motivated “confinement” radiator).

An important message comes from comparing the energy losses that occur at the hadronization stage. Based on the pickup hadronization picture, the characteristic parameter ϵ in (3.3) has been predicted to scale [9] as

$$\epsilon_Q \approx \left(\frac{m_q}{M} \right)^2 \propto M^{-2} \quad (3.15)$$

(with m_q the quantity of the order of the constituent light quark mass). Confronting (3.4) that (up to a logarithmic factor) scales as $\sqrt{\epsilon_Q}$ with the PT prediction (3.10), we get

$$\begin{aligned} \langle 1-x \rangle_{\text{fragm}} &\sim \sqrt{\epsilon_Q} \\ &\iff 1 - \langle x \rangle^{(C)} \\ &= 1 - \exp \left\{ -2C_F \frac{\mu_\alpha}{M} \right\} \\ &\approx 2C_F \frac{\mu_\alpha}{M}, \end{aligned}$$

which justifies the expected scaling law.⁸

⁸Similar behavior was advocated recently by Jaffe and Randall [26] who have exploited the difference between the hadron and heavy quark masses as a small expansion parameter.

It is worthwhile to remember that neither the Peterson function nor our PT-motivated “confinement” distribution is an unambiguously defined object. The former as an “input” for the evolution is by itself contaminated by gluon radiation effects at the hard scale $t \sim M^2$ that are present even at moderate $W \gtrsim 2M$. On the other hand, $D[k_\perp^2 \leq \mu^2]$ crucially depends on an arbitrarily introduced separation scale μ that disappears only in the product of the factors responsible for “PT” and “non-PT” stages (3.5a). Nevertheless, bearing this in mind, one may still speak of a direct correspondence between these two quantities, namely, $C(x)$ in the j representation and $D_j^{(C)}$ as given by (3.6).

This means that instead of convoluting phenomenological $C(x)$ with the W -dependent “safe” evolutionary quark distribution, one may try to use consistently the pure PT description that would place no artificial separator between the two stages of the hadroproduction. On first sight, one gains not much profit substituting one non-PT object, the phenomenological fragmentation function $C(x)$, with another unknown, namely, the behavior of the effective long-distance interaction strength $\alpha_s(k)$ (at, say, $k \lesssim 2 \text{ GeV}$). There is, however, an important physical difference between the two approaches: α_s should be looked upon as an *universal* process-independent quantity. Therefore quite substantial differences between inclusive spectra of c - and b -flavored hadrons should be under complete control according to the explicit quark mass dependence embodied in the PT formulas.

B. Modeling the coupling

To study the *infrared sensitivity* of PT results, one can try different shapes of the effective coupling or, equivalently, different ways to extrapolate the characteristic function

$$\xi(Q^2) = \int^{Q^2} \frac{dk^2}{k^2} \frac{\alpha_s(k)}{\pi} + \text{const} \quad (3.16)$$

to the ‘‘confinement’’ region of small Q^2 . Using the one-loop expression for the coupling,

$$\frac{\alpha_s^{(1)}(k)}{\pi} \equiv 2a^{(1)}(k^2) = \frac{4}{b \ln(k^2/\Lambda^2)}, \quad b = \frac{11}{3}N_c - \frac{2}{3}n_f, \quad (3.17)$$

for ξ , one gets

$$\xi^{(1)}(k^2) = \frac{4}{b} \ln \ln \frac{k^2}{\Lambda^2} + \text{const}, \quad (3.18)$$

which expression is defined only for $k > \Lambda$.

For the two-loop effective coupling, we use the standard approximate expression

$$\alpha_s^{(2)}(k) = \alpha_s^{(1)}(k) \left(1 - \frac{b_1 \ln \ln(k^2/\Lambda^2)}{4\pi b} \alpha_s^{(1)}(k) \right), \quad (3.19a)$$

with

$$b_1 = \frac{34}{3}N_c^2 - \left(\frac{10}{3}N_c + 2C_F \right) n_f \quad (3.19b)$$

and $\alpha_s^{(1)}$ given by the one-loop formula (3.17). The analytic expression for ξ then reads

$$\xi^{(2)}(k^2) = \frac{4}{b} \left(\ln L + \frac{b_1 \ln L + 1}{b^2 L} \right) + \text{const}, \quad L \equiv \ln \frac{k^2}{\Lambda^2}. \quad (3.20)$$

1. F model

The simplest prescription which we refer below as the *F* model consists of *freezing* the running coupling near the origin. One follows the basic PT dependence given by either (3.17) or (3.19a) down to a certain point k_c^2 where the coupling reaches a given value

$$\frac{\alpha_s(k_c)}{\pi} = A, \quad (3.21a)$$

and then keeps this value down to $k^2 = 0$. ξ then takes the form

$$= \xi(k^2) - \xi(k_c^2), \quad k^2 > k_c^2, \quad (3.21b)$$

$$\xi(k^2) = A \ln(k^2/k_c^2), \quad k^2 < k_c^2,$$

with k_c related to A by (3.21a).

2. G model

The set of G_p models (generalized shift models) gives another more flexible example for the trial effective coupling. It emerges when one regularizes the evolution function (3.18) as

$$\xi^{(1)}(k^2) = \frac{4}{b} \ln \ln \left(\frac{k^{2p}}{\Lambda^{2p}} + C_p \right) + \text{const}, \quad C_p \geq 1, \quad (3.22a)$$

which corresponds to the effective coupling

$$\begin{aligned} \frac{\alpha_s^{(1)}(k)}{\pi} &\equiv \frac{d\xi^{(1)}(k^2)}{d \ln k^2} \\ &= \left[\frac{k^{2p}}{k^{2p} + C_p \Lambda^{2p}} \right] \frac{4}{b} \frac{p}{\ln(k^{2p}/\Lambda^{2p} + C_p)}. \end{aligned} \quad (3.22b)$$

This expression preserves the perturbative asymptotic form (3.17) up to power corrections Λ^{2p}/Q^{2p} . Notice that the effective coupling (3.22b) with $C_p = 1$ has a finite limit $\alpha_s(0)/\pi = 4p/b$, while for $C_p > 1$ it vanishes at the origin.

For the two-loop coupling, one substitutes, in (3.20),

$$L \Rightarrow L_p = \frac{1}{p} \ln \left(\frac{Q^{2p}}{\Lambda^{2p}} + C_p \right), \quad (3.23a)$$

which results in

$$\begin{aligned} \frac{\alpha_s^{(2)}(k)}{\pi} &\equiv \frac{d\xi^{(2)}(k^2)}{d \ln k^2} \\ &= \left[\frac{k^{2p}}{k^{2p} + C_p \Lambda^{2p}} \right] \frac{4p}{bL_p} \left(1 - \frac{b_1 \ln L_p}{b^2 L_p} \right). \end{aligned} \quad (3.23b)$$

Trial shapes of the effective coupling in the G_2 model (G model with $p = 2$ and the two-loop α_s with $n_f = 5$ massless flavors) are displayed in Fig. 1 for different values of the parameter C_2 . Crosses mark the curve that provides the best fit to mean energy losses (see below).

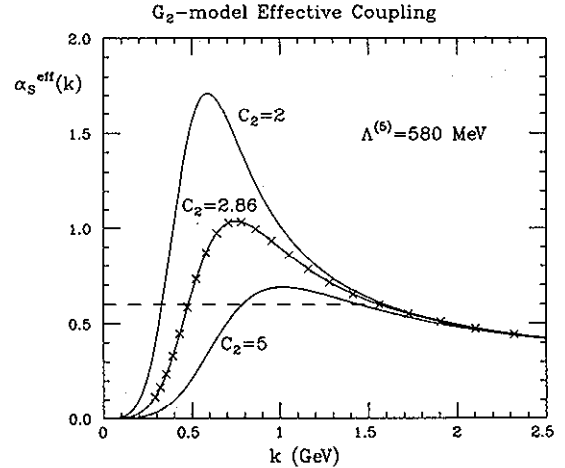


FIG. 1. Trial shapes of α_s^{eff} in the G_2 model (two loop, $n_f = 5$). Marked by crosses is the best-fit coupling. For comparison the best-fit *F*-model coupling ($A = 0.19$) is shown with a dashed line.

3. Quark thresholds

When it comes to an accurate account of heavy quark thresholds in α_s , we modify the logarithmic denominator of $\alpha_s^{(1)}(k^2)$ in (3.19a) according to (2.19) as

$$b_{[n_f=5]} \ln \frac{k^2}{\Lambda^2} \Rightarrow b_{[n_f=3]} \ln \frac{k^2}{\Lambda^2} - \frac{2}{3} \left[\Pi \left(1 + \frac{4M_c^2}{k^2} \right) + \Pi \left(1 + \frac{4M_b^2}{k^2} \right) \right], \quad (3.24a)$$

with

$$\Pi(v^2) = \frac{v(3-v^2)}{2} \ln \frac{1+v}{1-v} + v^2 - \frac{8}{3}. \quad (3.24b)$$

Given infrared regular behavior of α_s^{eff} , numerical evaluation of the inverse Mellin transform (2.4) with the PT radiator (2.7) becomes straightforward. The inclusive energy heavy quark spectrum obtained along these lines is concentrated (has a sharp maximum) near $x_Q = 1$ at $W \geq 2M$ and softens due to gluon bremsstrahlung effects with W increasing. One achieves a similar softening, increasing the radiation intensity in the PT domain (by taking a larger value of Λ) and/or at small momentum scales (by varying the “confinement parameter” of the model; larger A , smaller C_p).

Since available experimental information on differential heavy quark spectra is rather scarce at present (and possibly contradictory), we restrict ourselves by considering the *mean energy losses*, which, as we have discussed above, can be studied to quantify the influence of non-PT effects.

The value of $\langle x_Q \rangle \equiv D_2(W, M)$ shows quite a strong variation with A/C . However, from the general factorization argument (3.7a), one would expect the *energy dependence* of $\langle x_Q \rangle$ to stay well under PT control. As demonstrated in [27], the normalized quantity

$$\langle x_Q \rangle(W) / \langle x_Q \rangle(W_0) \quad (3.25)$$

is indeed practically insensitive to the variation of the “confinement parameter” of the model. Therefore the ratio (3.25) may be looked upon as an *infrared-stable* quantity suitable for measuring Λ as has been suggested by Mättig [1].

The position of the peak in the energy distribution seems to give another less trivial example of a stable prediction. Once again, as in the case of $\langle x_Q \rangle$, the *absolute* value of the peak position depends strongly on the chosen A value. At the same time the *normalized* quantity $x_{\text{peak}}(W)/x_{\text{peak}}(W_0)$ exhibits much weaker A/C dependence than the PT-controlled dependence on Λ [7,8].

Thus the W evolution (scaling violation) in quark energy losses $\langle x_Q \rangle(W)$ allows one to extract the scale parameter Λ which value proves to be practically insensitive to the adopted scheme of α_s^{eff} extrapolation. At the same time the *absolute* values of $\langle x_Q \rangle$ are quite sensitive to the gross effective radiation intensity below 1–2 GeV, which

makes it possible to quantify the corresponding “confinement parameter” of the scheme and, thus, the shape of the coupling.

It is worthwhile to notice that there is a natural theoretical scale, the “measurement” of α_s^{eff} below 1–2 GeV, to be compared to. As shown by Gribov [28], in the presence of light quarks color confinement occurs when the effective coupling (parameter A of the F model) exceeds rather *small* critical value

$$A > \left\{ \frac{\alpha_s}{\pi} \right\}^{\text{crit}} = C_F^{-1} \left[1 - \sqrt{\frac{2}{3}} \right] \approx 0.14. \quad (3.26)$$

Thus, within the Gribov confinement scenario, an interesting possibility arises. Namely, if phenomenological α_s^{eff} extracted from the data does exceed α_s^{crit} , but remains numerically small, this would provide a better understanding of the PT approach to multiple hadroproduction in hard processes.

IV. NUMERICAL ANALYSIS OF ENERGY LOSSES

In this section we compare experimental data with the generalized PT prediction which embodies the notion of the infrared regular effective QCD coupling. As an input we take the world average values [1] of $\langle x_Q \rangle$ listed in Table I. Errors have been evaluated by taking statistical and systematic errors in quadrature. The first three entries stand for the direct production of D^* mesons at different center-of-mass energies; the last four data for the mean *quark* energy have been extracted by unfolding the inclusive lepton (e, μ) spectra from heavy Q decays.

As mentioned above, the PT approach advocated in this paper cannot pretend to fully describe *exclusive* heavy hadron spectra (with D^* an example). Our treatment of the hadronization stage that implicitly appeals to duality arguments makes it plausible to rather apply this approach to inclusive quantities such as the lepton energy distributions. Nonetheless, for lack of anything better, we take the measured mean energy of D^* as a representative of $\langle x_Q \rangle$ to be compared directly with the PT-motivated prediction for the quark energy losses.

The preliminary analysis has shown [7,8] that an independent fitting of the D and L (epton) data results in the best-fit curves $A_D(\Lambda)$ and $A_L(\Lambda)$ that *cross* just at the best-fit value of Λ . This was the observation that

TABLE I. Experimental measurements of $\langle x_Q \rangle(W, M)$.

Process	$W_{\text{c.m.}}$ (GeV)	$\langle x_Q \rangle$
(1)	10.4	0.727±0.014
(2) $c \rightarrow D^* + \dots$	30	0.587±0.015
(3)	91	0.508±0.009
(4) $c \rightarrow l + \dots$	57.8	0.541±0.036
(5) $c \rightarrow l + \dots$	91	0.522±0.022
(6) $b \rightarrow l + \dots$	29–35	0.789±0.022
(7) $b \rightarrow l + \dots$	91	0.699±0.009

motivated us to look upon α_s^{eff} as a process-independent quantity to confront the c and b measurements 1–7 with a unique one-parameter PT prediction.⁹

Hereafter, we fix heavy quark masses to be

$$M_c = 1.5 \text{ GeV}, \quad M_b = 4.75 \text{ GeV}. \quad (4.1)$$

(Sensitivity to the b -quark mass will be discussed below.)

A. Fitting mean quark energies

Figure 2 shows the quality of the fit to seven separate data of Table I together with the total χ^2 as a function of $\Lambda^{(5)}$ in the F model with $A = 0.191$ (the best-fit value). Some explanation is in order. In this figure (and similar plots below) for each datum the ratio

$$\frac{\text{theor} - \text{expt}}{\text{expt error}} \quad (4.2)$$

is displayed against the right vertical scale. Dashed horizontal lines mark 1σ levels for each single datum. The two curves (which should be read out against the left scale) show the squared deviation of the points (4.2) from the median, that is, the total χ^2 . The solid curve sums up all seven data, while the dash-dotted one accumulates the “high W ” data only. The “high W ” sample we define excluding the entries No. 1 and No. 6, which correspond to the quark mass-to-energy ratios

$$M/E \approx M_c/5 \text{ GeV} \sim M_b/15 \text{ GeV} \approx \frac{1}{3}.$$

These two entries are subject to significant nonrelativistic corrections. The fact that the two fits are consistent is good news: It shows that the nonrelativistic effects have been properly taken into account¹⁰ in the PT radiator (2.7).

Figure 3 demonstrates sensitivity of the PT description to the “confinement parameter.” Here we have chosen the G_2 model for a change. The first thing to be noticed is that with the best-fit parameter $C_2 = 2.86$ one obtains the same value $\Lambda^{(5)} \approx 580 \text{ MeV}$, a comparable quality of the fit, $\chi_{\text{min}}^2 \approx 0.7$, and even the same dynamics of each of seven data as in the above F -model description (Fig. 2). In the upper part of this plot, two marginal values of C_2 are also shown which correspond to one standard deviation from the total seven-fit: $\chi_{\text{min}}^2(2.53) = \chi_{\text{min}}^2(3.21) = \chi_{\text{min}}^2(2.86) + 1$.

In Fig. 4 comparison is made of the quality of the fits within different models for the effective coupling (two loop, $n_f = 5$). For each value of Λ , the A/C parameter

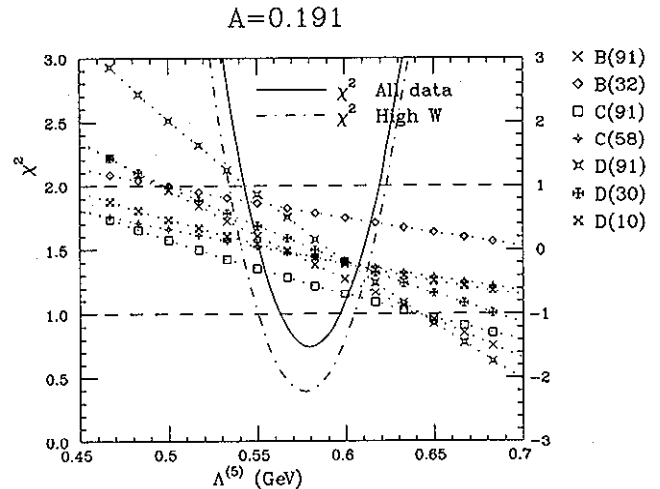


FIG. 2. Λ dependence of the F -model fit to mean energy losses (two-loop α_s^{eff} with $n_f = 5$). The right scale shows the normalized deviation between a theoretical prediction and an experimental datum (4.2). Dashed lines mark the 1σ band. Solid and dash-dotted lines show the values of χ^2 (against the left scale) for all data and the high W data sample correspondingly.

has been adjusted to minimize the error (one-parameter fit). The upper scale shows corresponding values of $\alpha_{\overline{\text{MS}}}$ at LEP recalculated from α_s^{eff} with use of the relation (2.17b).

It is worthwhile to notice some peculiarity of the G_1 model. This model is “too soft” in a sense that it induces the *negative* preasymptotic power term $\propto k^{-2}$ in $\alpha_s^{\text{eff}}(k)$, which correction suppresses α_s^{eff} in a relatively high momentum region.

Figure 5 illustrates this peculiarity. Here the couplings corresponding to the best-fit A/C values for $\Lambda^{(5)} = 580 \text{ MeV}$ are compared. Solid lines (F, G_{2-4}) correspond to $\chi^2 \approx 0.7$. In the G_1 model shown by the dash-dotted line ($\chi^2 \approx 1.2$), α_s^{eff} stays noticeably smaller above 1.5 GeV before the perturbative logarithmic regime sets up and all the models merge.

As a result, to compensate for reduced radiation intensity the best-fit Λ value [and thus $\alpha(M_Z)$] within the G_1 model tends to be larger compared to “sharp” models F, G_2, \dots

Leaving G_1 aside, we conclude that both the quality of the fit and the value of Λ the “sharp” models point at hardly exhibit any model dependence. From Fig. 4 (see also Fig. 3) we deduce

$$\Lambda^{(5)} = 580 \pm 80 \text{ MeV}. \quad (4.3a)$$

Being translated into the $\overline{\text{MS}}$ parameter this gives

$$\alpha_{\overline{\text{MS}}}(M_Z) = 0.127 \pm 0.003. \quad (4.3b)$$

The error here is purely statistical (one standard deviation).

⁹In spite of the fact that such a naive approach suggests the same theoretical expectation for the two physically different data No. 3 and No. 5.

¹⁰The relativistic version of (2.4)–(2.7) reported earlier [7] failed to properly embody the “ b at 32” datum No. 6.

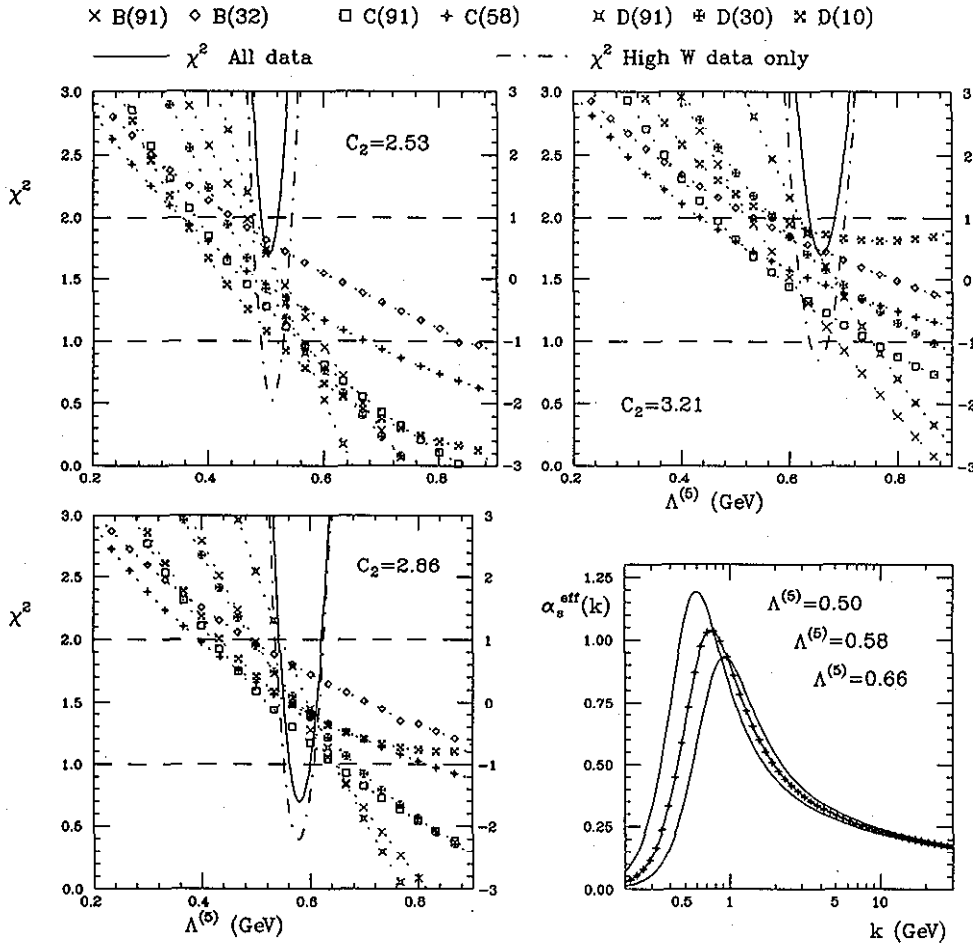


FIG. 3. Sensitivity of the G_2 -model fit to the shape of α_s^{eff} at the origin (two loop, $n_f = 5$). The values of C_2 in the upper plots correspond to one standard deviation from the best fit (bottom-left). The bottom-right graph displays the margin in the low-momentum behavior of α_s^{eff} .

In what follows we shall be using the 0.003 shift in $\alpha_{\overline{\text{MS}}}(M_Z)$ induced by the G_1 model (see Fig. 4 and Table II below) as a rough estimate of the systematic uncertainty due to possible "soft" preasymptotic power effects in the running coupling.

Figure 6 demonstrates consistency of the total G_2 -model fit with fits to various subsets of data: D^* (items

1-3 of Table I), "leptons" (4-7), high W (items 2-5, 7). Here χ^2 is plotted against the reference value $\alpha_{\overline{\text{MS}}}(M_Z)$.

D^* data are more restrictive since they have smaller experimental errors than inclusive lepton measurements. Low W points $b \rightarrow \text{leptons} + \dots$ at 32 (No. 6) and, especially, D^* at 10 (No. 1) are quite important as they provide a lever arm for scaling violation. Inclusion of

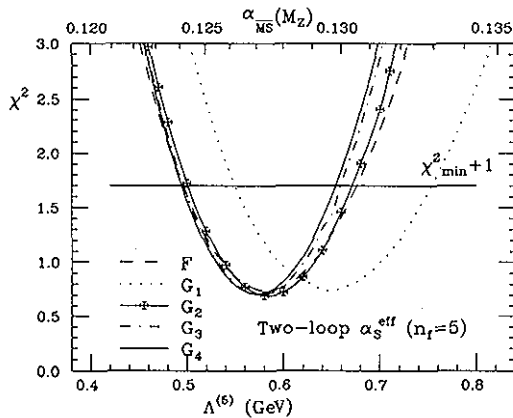


FIG. 4. One-parameter fits to energy losses within different models for α_s^{eff} .

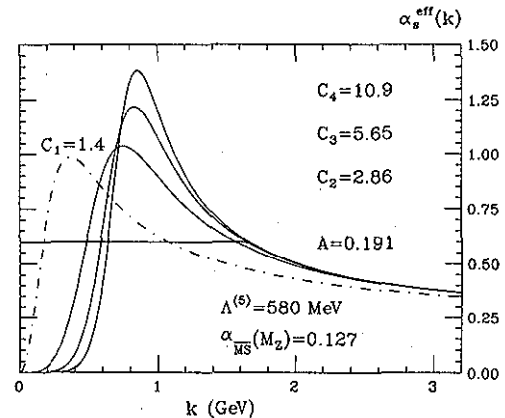


FIG. 5. Best-fit α_s^{eff} for $\Lambda^{(5)} = 580$ MeV. The G_1 model underestimates the radiation above 1.5 GeV.

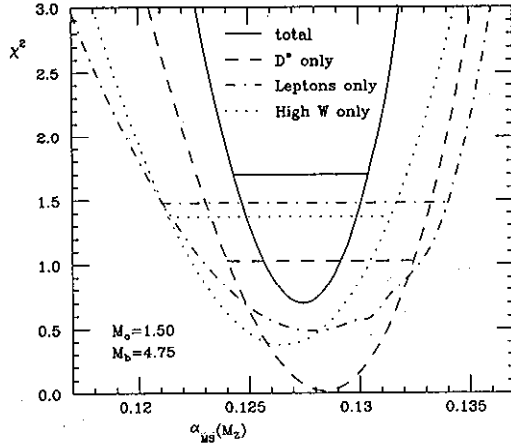


FIG. 6. Consistency between the fits to different subsets of data on mean energy losses (two loop, $n_f = 5$). Horizontal lines mark one standard deviation levels.

these two measurements does not spoil the fit, $\chi^2/5$ (total fit) $\approx \chi^2/3$ (high W), but increases its quality reducing statistical error by a factor of 2.

B. Energy ratios and Λ determination

In Fig. 7 results of the G_1 -model fit to the ratios of $\langle x_Q \rangle$ at different energies are shown. Solid curves accumulate the squared errors in the description of four ratios $D^*(91)/D^*(10)$ and $D^*(91)/D^*(30)$ and two ratios from leptonic quark decays, $C(91)/C(58)$ and $B(91)/B(32)$. As we have discussed above, one expects such ratios to

be protected against our ignorance about the confinement physics. Indeed, a rather high stability in the quality of the fit inside a huge range of variation of the "confinement parameter" C_2 is seen. Bottom-right insertion displays the corresponding shapes of α_s^{eff} . Within the chosen interval of C_2 , the characteristic value of $\bar{\Lambda}$ (4.6) varies from 0.09 ($C_2 = 10$, $\Lambda = 0.7$) up to 0.41 ($C_2 = 1.4$, $\Lambda = 0.5$), that is, changes by a factor of 2 in both directions around the value 0.19 [Eq. (4.6b)] that we have obtained describing *absolute* energy losses.

Also shown in Fig. 7 is the mixed bottom-to-charm ratio $B(91)/C(91)$. This one does not belong here and, contrary to the generic c/c and b/b quark ratios, strongly depends on C_2 as expected.

We observe that three of four generic ratios show no variation with C_2 at all. It is the ratio $D^*(91)/D^*(10)$ only that induces some *negative* correlation between $\bar{\Lambda}$ and Λ : The latter moves to larger values with a decrease of the low-scale interaction intensity. Such a systematic drift is natural: The charm quark mass is too small to completely protect the normalization point $D^*(10)$ against W -dependent (*sic*) confinement effects at total energy as low as 10 GeV. At the same time the first ratio dominates the fit, while the experimental accuracy of the three others is not sufficient at present to provide a direct safe way of measuring the Λ parameter.

Roughly, one might present the result of fitting quark energy ratios as

$$\Lambda^{(5)} = 0.60 \pm 0.15(\text{stat}) \pm 0.10(\text{syst}). \quad (4.4a)$$

If statistical and systematic errors in Fig. 7 were uncorrelated (which is not the case), (4.4a) would correspond to

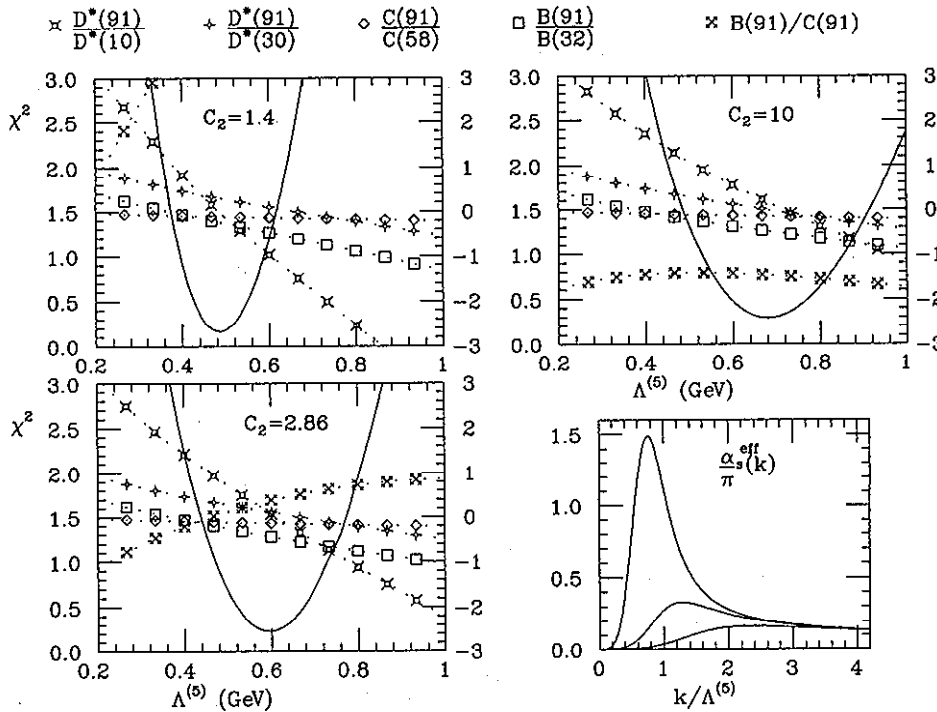


FIG. 7. C_2 dependence of energy ratios (G_2 model, two loop, $n_f = 5$) with χ^2 for the first four ratios shown by solid lines and corresponding shapes of α_s^{eff} (bottom-right). The ratio $B(91)/C(91)$ not belonging to the fit exhibits a strong C_2 dependence, contrary to generic c/c and b/b ratios.

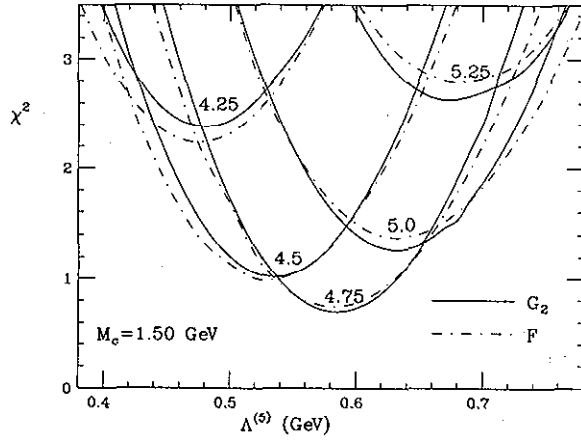


FIG. 8. M_b dependence. Fits within F and G_2 models are shown (two loop, $n_f = 5$).

$$\alpha_{\overline{\text{MS}}}(M_Z) = 0.128 \pm 0.007. \quad (4.4b)$$

For the time being it will suffice to conclude that determination of $\Lambda^{(5)}$ from quark energy ratios is consistent with that from absolute energy losses; cf. (4.3).

C. Bottom quark mass

Figure 8 illustrates sensitivity of the total seven-fit to the bottom quark mass. Here we have fixed $M_c = 1.5$ GeV and looked for a minimal χ^2 with respect to variation of A/C_2 (one-parameter fit) for a given Λ and M_b .

The quark mass dependence of the spectrum (2.4)–(2.7) and, thus, of energy losses is basically logarithmic [apart from nonrelativistic corrections $(M/W)^2$ and “confinement” effects μ_α/M]. Nevertheless, a certain range of “preferable” bottom quark masses may be read out from Fig. 8. Within one standard deviation (G_2 model),

$$M_b = 4.73 \pm 0.38 \text{ GeV}. \quad (4.5)$$

A better understanding of the nature of the mass parameter M as it enters the PT formulas is needed before such an analysis may be used for “measuring” the bottom quark mass.

As for now, one finds satisfaction in noticing that the value $M_b = 4.75$ GeV we have been using throughout this paper [29] does fit nicely into the PT picture of mean energy losses.

D. Integrated coupling as invariant of the fit

Being free to play around with the detailed shape of α_s^{eff} at the origin, one finds it necessary at the same time to fix some characteristic measure of the radiation intensity in the non-PT momentum region. Figure 5 suggests trying an *area* under the curve for an invariant parameter of the fit. The result is quite impressive: Areas under the G_{2-4} and F couplings are practically indistinguishable. Introducing

$$\bar{A}(\mu) \equiv \frac{1}{\mu} \int_0^\mu dk \frac{\alpha_s^{\text{eff}}(k)}{\pi}, \quad (4.6a)$$

TABLE II. Best seven-fits within various models for effective coupling. A/C , $\alpha_{\overline{\text{MS}}}$, χ^2 , and \bar{A} are given for the central Λ values.

Model for α_s^{eff}	Best fit parameter	Λ (MeV)	$\alpha_{\overline{\text{MS}}}(M_Z)$	χ^2 5 DF	Integral \bar{A} (4.6b)
Two-loop, with c, b thresholds; $\Lambda^{(3+2)}$	$A = 0.184$	730 ± 95	0.125	0.66	0.184
	$C_2 = 2.48$	725 ± 85	0.125	0.64	0.191
	$C_3 = 4.41$	710 ± 80	0.124	0.66	0.193
	$C_4 = 7.79$	705 ± 80	0.124	0.68	0.194
	$C_1 = 1.38$	820 ± 100	0.128	0.69	0.189
Two-loop, with five massless quarks; $\Lambda^{(5)}$	$A = 0.190$	585 ± 85	0.127	0.73	0.187
	$C_2 = 2.88$	585 ± 80	0.127	0.68	0.191
	$C_3 = 5.59$	575 ± 80	0.127	0.69	0.193
	$C_4 = 10.8$	575 ± 75	0.127	0.70	0.193
	$C_1 = 1.46$	655 ± 95	0.130	0.75	0.190
One-loop, with three massless quarks; $\Lambda_{\text{one loop}}^{(3)}$	$A = 0.193$	480 ± 70	0.120	0.71	0.188
	$C_2 = 2.22$	485 ± 65	0.120	0.66	0.190
	$C_3 = 3.94$	480 ± 60	0.120	0.66	0.191
	$C_4 = 6.90$	480 ± 60	0.120	0.66	0.191
	$C_1 = 1.20$	515 ± 75	0.122	0.69	0.189
One-loop, with five massless quarks; $\Lambda_{\text{one loop}}^{(5)}$	$A = 0.209$	310 ± 50	0.133	0.90	0.189
	$C_2 = 2.68$	315 ± 50	0.133	0.79	0.191
	$C_3 = 5.48$	315 ± 50	0.133	0.78	0.191
	$C_4 = 10.9$	315 ± 50	0.133	0.79	0.191
	$C_1 = 1.28$	330 ± 50	0.134	0.84	0.189

we get (with one standard deviation error estimated from the G_2 -model margin; see Fig. 5)

$$\bar{A}(2 \text{ GeV}) = 0.190 \pm 0.010. \quad (4.6b)$$

This integral measure not only proves to be quite stable against the choice of *low*-momentum regularization, but also resistant to different approximations for the *high*-momentum tail of $\alpha_s^{\text{eff}}(k)$.

Table II accumulates characteristics of various seven-fits and demonstrates an amusing stability of the value (4.6b). This justifies the qualitative expectation of Sec. III A that it is the integral of the coupling as a characteristic measure of confinement (hadronization) effects in inclusive energy spectra, μ_α of Eq. (3.9), that is responsible for the low-momentum contribution to mean energy losses.

Thus we find empirically that the characteristic integral (4.6) turns out to be a *fit-invariant* quantity which one has to keep fixed to describe the absolute values of energy losses. As pointed out by Gribov, it can be looked upon as the long-distance contribution to the QCD field energy of a heavy quark. It is worthwhile to notice that such an integral appears in the relation between the running heavy quark mass at scale μ and the pole mass [30]

$$\begin{aligned} M^{\text{pole}} - M(\mu) &= \frac{8\pi}{3} \int_{|\vec{k}| < \mu} \frac{d^3 k}{(2\pi)^3} \frac{\alpha_s(k)}{k^2} \\ &= C_F \int_0^\mu d\kappa \frac{\alpha_s(\kappa)}{\pi} \\ &\equiv C_F \mu_\alpha. \end{aligned} \quad (4.7)$$

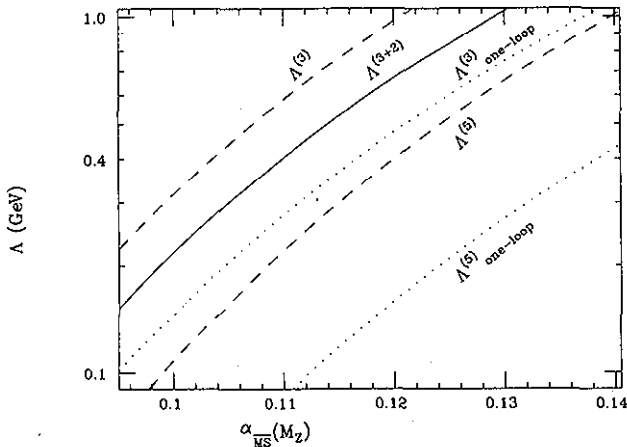


FIG. 9. Relation between Λ and $\alpha_{\overline{\text{MS}}}(M_Z)$: one loop (dotted line), two loop (dashed line) for three and five massless quarks and the two-loop coupling with c - and b -quark thresholds (solid line).

E. Two-loop α_s^{eff} with heavy quark thresholds and $\alpha_{\overline{\text{MS}}}$ determination

It is important to notice that the different approximations for the high-momentum tail of α_s^{eff} listed in Table II provide similar quality fits and preserve the \bar{A} value, but at the same time lead to systematically different values of $\alpha_{\overline{\text{MS}}}(M_Z)$. Figure 9 helps to relate the values of the Λ parameter for different approximations for the running α_s^{eff} to the reference value $\alpha_{\overline{\text{MS}}}(M_Z)$.

In the problem under consideration, one probes the coupling at M_Z scale only indirectly. To start, "half" of the data belong to smaller W 's. Moreover, even when the LEP measurements are concerned, the main contribution to energy losses originates from a broad logarithmic integral of $\alpha_s^{\text{eff}}(k)$ running from $k \lesssim M_Q$ up to $k \lesssim M_Z$, so that momenta just above M_b (as well as between M_c and M_b) play quite an essential role. The reference values of $\alpha_{\overline{\text{MS}}}$ appearing in Table II emerge as a result of extrapolation from intermediate momentum scales that dominate in the fit. Such an extrapolation is sensitive to details of the high-momentum behavior of the running coupling. When n_f is taken smaller and/or the two-loop effects are being taken into account, α_s^{eff} becomes a steeper falling function of momentum and the resulting value of $\alpha_{\overline{\text{MS}}}(M_Z)$ decreases.

Even an account of heavy quark thresholds [which makes $\alpha_s^{\text{eff}}(k)$ a steeper function below $k \lesssim M_b$] drives down the $\alpha_{\overline{\text{MS}}}$ value. To demonstrate this effect we include Figs. 10 and 11, showing the quality of the PT description of absolute energy losses with an account of the second loop and c - and b -quark threshold effects in the running coupling. In Fig. 10 the model dependence of the total seven-fit is shown (cf. Fig. 4); Fig. 11 collects fits to different subsets of data (cf. Fig. 6).

Our conclusions about the relative stability against the choice of low-momentum regularization model and about the consistent description of leptonic, D^* , and high W data hold. From these plots one obtains (see also Table II)

$$\Lambda^{(3+2)} = 0.720 \pm 0.080(\text{stat}) \pm 0.015(\text{syst}) \text{ GeV}, \quad (4.8a)$$

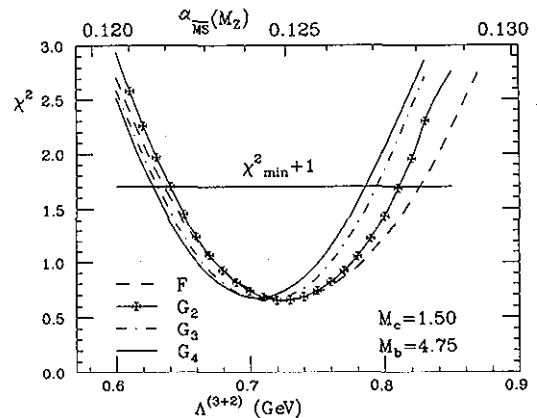


FIG. 10. Quality of the total fits vs Λ (two-loop α_s^{eff} with c , b thresholds).

TABLE III. Characteristics of the best G_2 -model fits.

G_2 model	n_f	$\Lambda^{(n_f)}$	C_2	χ^2	\bar{A} (2 GeV)	α_s^{eff} (2 GeV)	$\alpha_s^{\text{eff}}(M_b)$	$\alpha_s^{\text{eff}}(M_Z)$	$\alpha_{\overline{\text{MS}}}(M_Z)$
+thresholds	3+2	725	2.48	0.65	0.191	0.530	0.303	0.135	0.125
	5	315	2.68	0.79	0.191	0.443	0.302	0.145	0.133
One-loop	4	395	2.43	0.72	0.191	0.463	0.303	0.139	0.126
	3	485	2.22	0.66	0.190	0.488	0.306	0.134	0.120
	5	585	2.88	0.69	0.191	0.494	0.303	0.138	0.128
Two-loop	4	770	2.72	0.64	0.190	0.549	0.305	0.131	0.120
	3	935	2.56	0.62	0.190	0.608	0.305	0.124	0.112

where we have singled out systematic uncertainty due to model dependence. This results in

$$\alpha_{\overline{\text{MS}}}(M_Z) = 0.125 \pm 0.003. \quad (4.8b)$$

It is important to stress that the second loop effects are there in the running coupling and n_f is not a free parameter: Quarks (and their masses) are what they are. Therefore a huge interval of $\alpha_{\overline{\text{MS}}}$ values seen in Table II has nothing to do with the actual theoretical uncertainty in determining this important datum.

Before we turn to a discussion of systematic errors, some comment is in order. It has to do with the number of acting quark flavors and will eventually give us an additional consistency check of the approach.

An attentive reader could have noticed that using five-flavor running coupling seems to contradict the very logic of the present paper. Indeed, in Sec. II we constructed the energy distribution corresponding to *direct* production of a heavy quark Q . To do so we disregarded the sea mechanism of heavy quark production and omitted the second loop anomalous dimension term related to $Q\bar{Q}Q\bar{Q}$ final states.

However, there is yet another subtle source of copious $Q\bar{Q}$ pairs, namely, the running coupling α_s^{eff} embodied

into the PT radiator. The way the coupling runs in theoretical expressions for inclusive characteristics depends on the experimental setup: A veto on fermion pair production in the final state suppresses the effective interaction strength at large momentum scales (QCD coupling decreases faster; an increase of α_{em} slows down). Therefore, to preserve the logic of the approach, we better make it clear that the use of the $n_f = 3$ effective coupling, which goes along with the suppression of additional $c\bar{c}, b\bar{b}$ pairs, is consistent with the reported result (4.8b).

In Fig. 12, G_2 -model couplings are shown with the best-fit parameters Λ and C_2 listed in Table III. As far as low momenta are concerned, variations due to n_f and one versus two loops should be looked upon simply as different models for trial-regularized coupling. All of them do the job. In particular, the three-flavor α_s^{eff} which interests us at the moment (the last line of Table III) does

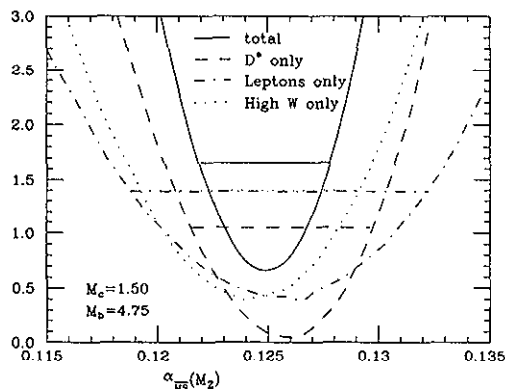


FIG. 11. Consistency of G_2 -model fits to subsets of data (two loop; c, b thresholds).

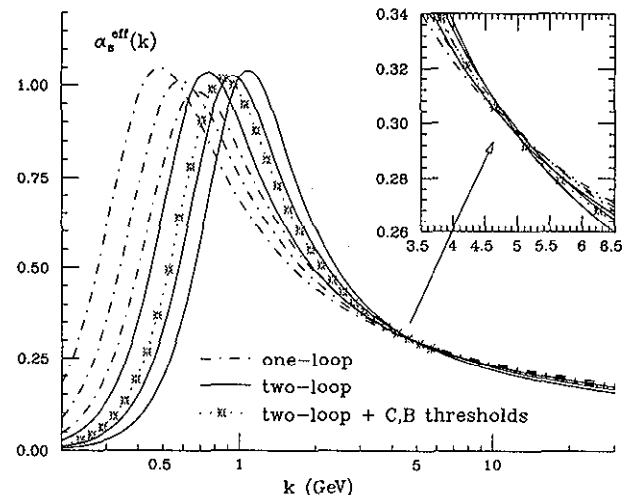


FIG. 12. G_2 -model couplings with the best-fit parameters Λ and C_2 listed in Table III. As far as low momenta are concerned, variations due to n_f and one vs two loops should be looked upon simply as different models for trial-regularized coupling. All of them do the job. In particular, the three-flavor α_s^{eff} which interests us at the moment (the last line of Table III) does provide an excellent fit, $\chi^2/N_{\text{DF}} \approx 0.6/5$.

provide an excellent fit, $\chi^2/N_{DF} \approx 0.6/5$.

High stability of the \bar{A} value (4.6b) is confirmed once again. Moreover, one more interesting fit-invariant quantity emerges, namely, the value of the effective coupling at the bottom mass scale:¹¹

$$\alpha_s^{\text{eff}}(M_b) \approx 0.30. \quad (4.9)$$

The curves in Fig. 12 are quite different below 2 GeV, focus around 5 GeV, and diverge again at high momenta. The columns adjacent to the double-lined one in Table III illustrate this behavior. In particular, the three-flavor coupling continued to the LEP scale is substantially lower compared to the "3+2" coupling we have been using before (0.124 vs 0.135). However, it would be erroneous to read out $\alpha_{\overline{\text{MS}}}(M_Z) = 0.112$ from the last line of Table III.

As we see, heavy flavors in α_s^{eff} are indeed irrelevant for the problem under consideration. However, they do contribute to the evolution of the standard QCD coupling. Therefore, having found the magnitude of α_s^{eff} at intermediate scales $k \sim 5$ GeV which dominate in the problem, one has to apply the five-flavor evolution from ~ 5 up to 91 GeV, aiming at extraction of the reference value $\alpha_{\overline{\text{MS}}}(M_Z)$.

Since the starting value $\alpha_s^{\text{eff}}(M_b) = 0.305$ practically coincides with that from the previous "3+2" analysis (0.303), so do the results. Choosing the starting point of high-momentum extrapolation in between $k = M_b/2$ and $k = 2M_b$ leads to

$$\alpha_{\overline{\text{MS}}}(M_Z) = 0.125 \pm 0.003. \quad (4.10)$$

The, slightly inflated, error here is moderate, and the central value perfectly matches with the result of the previous analysis (4.8b) based on "3+2" coupling.

F. Systematic errors and prospects

First of all, there is a problem of the correspondence between theoretical predictions and the data. As we have stressed above, the formulas of this paper were designed to describe the mean energy of a primary quark produced in the e^+e^- annihilation vertex. We were treating experimental numbers as corresponding to direct $Q\bar{Q}$ production. We do not feel in a position to judge to what extent the experiments actually met such an expectation.

The good news is, however, that the bottom sector is safe in this respect: The $g \rightarrow b$ sea component is vanishingly small at present and so is charm production at low energies [31]. Therefore only LEP charm data should concern us here. Bearing this in mind, it is important to notice that the D^* LEP datum No. 3 (which is the most precise measurement and therefore practically the only

one vulnerable) does correspond to primary charm.¹² Monte Carlo (MC) modeling was used to subtract the gluon component (with an uncertainty included in the experimental systematic error). The reliability of such a subtraction has been recently verified by the first OPAL measurement of the charm production via gluons [32].

Apart from this, one can think of the following sources of systematic error of $\alpha_{\overline{\text{MS}}}(M_Z)$ determination.

(1) *Higher orders. Estimate: 0.002; Comment: optimistic.* follows from analysis of the approximate relation (2.17b) between physical coupling α_s^{eff} and $\alpha_{\overline{\text{MS}}}$ and of forceful exponentiation of α_s terms in the radiator (2.7). Apart from the three-loop analysis, an exact $O(\alpha_s^2)$ theoretical calculation of $\langle x_Q \rangle$ would be helpful.

(2) *Power effects in α_s^{eff} ($k > 2$ GeV). 0.003; arbitrary (hopefully conservative).* is based on comparison with the "soft" G_1 model (see above). The variation within "hard" regularization models (F, G_{2-4}) is below 0.001 [see (4.8)]. To gain quantitative theoretical control over the $1/k^2$ power term in the effective coupling and, thus, to reduce corresponding systematic error might be not as hopeless a goal as it seems.

(3) *Kinematical effects. 0.000; safe.* The structure of the PT spectrum is such that it respects the kinematical boundary $x \geq x_{\min} = 2M/W$ only in the first α_s order. The contribution to $\langle x_Q \rangle$ from the potentially dangerous region between x_{\min} and $2x_{\min}$ can be estimated as

$$\Delta \langle x_Q \rangle \sim \alpha_s(W)/\pi(1 - \langle x_Q \rangle)x_{\min}^2,$$

which value is well below 1% even for x_{\min} as big as $\frac{1}{3}$.

(4) *Quark masses. 0.002; conservative.* Given that the structure of the low-momentum contribution proportional to \bar{A} naturally embodied in PT analysis reminds that of the shift from Euclidean to "on-shell" quark mass [see (4.7)], one may worry about *double counting* if the pole mass is used for M in the PT formulas. The problem should be studied theoretically. Meanwhile, let us mention that one may get an equally good description of the absolute values of mean quark energy losses with *smaller* (Euclidean?) quark masses plugged in. For example, by taking

$$M_c = 1.30 \text{ GeV}, \quad M_b = 4.50 \text{ GeV},$$

one obtains¹³

G_2 model	C_2	χ^2	\bar{A} (2 GeV)	$\alpha_{\overline{\text{MS}}}(M_Z)$
$\Lambda^{(5)} = 600$	3.60	0.72	0.166	0.1280
$\Lambda^{(3+2)} = 740$	2.94	0.66	0.166	0.1257

We observe that the resulting value $\alpha_{\overline{\text{MS}}}(M_Z)$ hardly increases by 1 per mil.

¹¹Since the magnitude of α_s^{eff} around 5 GeV $\gg \Lambda$ is insensitive to A/C and depends only on Λ , the same conclusion (4.9) follows from F and $G_{3,4}$ models.

¹²An older average $\langle x_{D^*} \rangle = 0.494 \pm 0.014$, which we have used in the previous analysis [27], was contaminated by the sea. We are indebted to P. Mättig for clarifying this point.

¹³4.5 is a preferable bottom mass value for $M_c = 1.3$, analogously to $M_b = 4.75$ for $M_c = 1.5$; see above, Fig. 8.

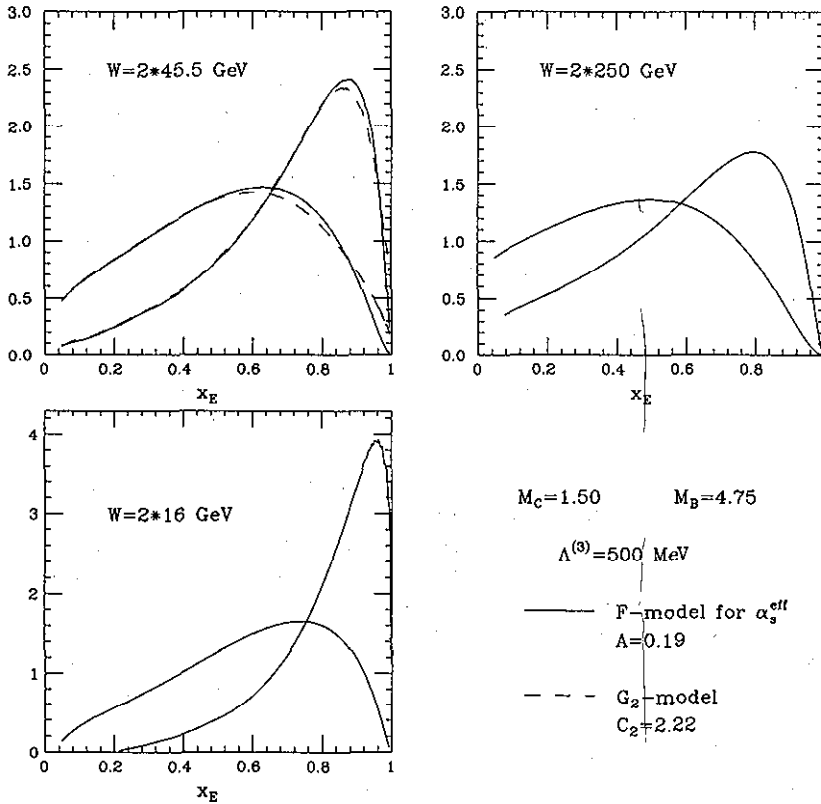


FIG. 13. Evolution of inclusive c, b spectra from $W = 32-500$ GeV. The best-fit F -model (solid line) and G_2 -model curves (dashed line) are shown.

Another feature of the alternative set of quark masses worth noticing is a systematic decrease of the value of characteristic integral \bar{A} . This may be a welcome trend bearing in mind a recent analysis of power corrections to jet shape variables; see [33]. For the time being we choose to look upon this 10% shift as a systematic uncertainty which will be greatly reduced when proper theoretical understanding of the nature of the quark mass parameter is achieved.

Having said that, we modify (4.6b) and present the final result for the integrated coupling as

$$\bar{A}(2 \text{ GeV}) = 0.18 \pm 0.01(\text{stat}) \pm 0.02(\text{syst}). \quad (4.11)$$

Finally, in Fig. 13 we demonstrate the W evolution of realistic c - and b -quark spectra obtained within the F model with one-loop three-flavor α_s^{eff} . These curves correspond to the values of A and Λ providing the best common fit to mean energy losses as described above. For comparison the best-fit G_2 -model curves are also shown for LEP energy. F - and G -model spectra are quite close to each other. We may conclude that it suffices to fix the integral parameter (4.6b) together with the value of Λ to predict the differential energy distributions with a reasonable accuracy.¹⁴

A stable numerical procedure for numerical evaluation

of the inverse Mellin transform (2.4) remains to be designed.

V. CONCLUSIONS

Jets initiated by heavy quarks (b, c) are now extensively studied experimentally. The interest in this subject is connected not only with testing the fundamental aspects of QCD, but also with its large potential importance for measurements of heavy particle properties: lifetimes, spatial oscillations of flavor, searching for CP -violating effects in their decays, etc. Properties of b -initiated jets are of primary importance for analysis of the final state structure in the $t\bar{t}$ production processes.

In this paper we presented results of the study of the inclusive energy spectra of leading heavy flavored particles (H_Q) based on the perturbative expressions (2.4)–(2.7) for heavy Q distributions that emerge after taking into proper account multiple gluon bremsstrahlung off the $Q\bar{Q}$ pair.

Our approximation includes the two-loop anomalous dimension, keeps track of the *collinear* logarithms $a \ln W$ and $a \ln M$, *soft* double-logarithmic $a \ln^2(1-x_Q)$, and essential single-logarithmic $a \ln(1-x_Q)$ contributions in all orders. At the same time, it embodies the exact first order result $O(a)$ for the inclusive energy distribution, which property is necessary to account for nonrelativistic suppression of gluon radiation in the situation when jet energies are comparable with a heavy quark mass.

The spectra we have been considering correspond to *direct* Q production. Such an approach disregards the

¹⁴Let us notice that the differential quark energy spectra obtained by the inverse Mellin transform (2.4), (2.6) violate kinematical boundary $D(x < 2M/W) = 0$ at the $O(\alpha_s^2)$ level.

sea contribution to heavy quark yield, which is numerically small at present and foreseeable energies. Accordingly, a specific term in the nonsinglet two-loop anomalous dimension has been omitted which is due to $QQ\bar{Q}\bar{Q}$ final states and would violate the “multiplicity” sum rule (2.1).

Apart from this simplification, the formal relative accuracy of the perturbative result (2.4)–(2.7) is $O(a^2(W^2))$, which estimate is *uniform* in x_Q . Perturbative corrections at the quark mass scale which were left out of control start from $O(a^3(M^2))$.

We have formulated the perturbative result (2.4)–(2.7) in terms of a “physical” coupling, the one which directly measures radiation intensity of relatively soft gluons [21]. This coupling constant is different from (roughly, 10% larger than) $\alpha_{\overline{MS}}$ and is approximately related to the latter by (2.17b). Expressed in terms of α_s^{eff} , the radiator (2.7) acquires the two-loop contribution $\hat{\Delta}^{(2)}$, which is free from an artificial n_f dependence [22] and proves to be numerically negligible.

There are two ingredients of the standard approach to description of H_Q spectra. Here one starts from the phenomenological non-PT fragmentation function for the $Q \rightarrow H_Q$ transition and then traces its evolution with an increase of the annihilation energy W by means of PT QCD. Being formally well justified for describing the W evolution, this approach, however, leaves the dependence on the quark mass M basically out of the PT control.¹⁵

Motivated by the LPHD concept, we attempted to derive *pure* PT predictions without invoking the phenomenological fragmentation function. The starting point for such an attempt was the observation that an appearance of the parton model motivated *peak* in the non-PT fragmentation at large x_Q [25,9] can be attributed to the Sudakov suppression effects *provided* one feels courageous enough to continue the PT description down to the region of gluon transverse momenta, $k_{\perp} \sim \Lambda(W/\sqrt{M\Lambda})^{0.2}$, which at present (and foreseeable) energies looks dangerously close to the nonperturbative domain.

When getting rid of the transverse momentum cutoff, one faces the problem of the formal “infrared pole” in α_s and is forced to introduce the effective nonsingular coupling $\alpha_s^{\text{eff}}(k)$ that remains finite at $k \leq \Lambda$. It is not easy to justify the very notion of α_s at small momenta where the PT quark-gluon language seems to be hardly applicable at all. In the problem under consideration, it can be related to the effective measure of intensity of accompanying particle production at the confinement stage of the H_Q formation, a finite number of light hadrons produced in addition to the (W -dependent) particle yield due to PT-controlled gluon bremsstrahlung at the first stage of the hard $Q\bar{Q}$ pair creation process.

We have checked that, in accordance with expecta-

tions based on general factorization properties, our ignorance about confinement does not affect the W dependence of the mean energy losses $\langle x_Q \rangle(W, M)$. Thus the ratio $\langle x_Q \rangle(W)/\langle x_Q \rangle(W_0)$ can be used to extract the fundamental QCD parameter Λ . Another infrared-stable quantity found empirically is the PT prediction for the normalized peak position, $x_Q^{\text{peak}}(W)/x_Q^{\text{peak}}(W_0)$.

At the same time, the absolute values of $\langle x_Q \rangle$, peak positions, and particle distributions in general show up substantial variations with the value (momentum dependence) of α_s^{eff} in the origin chosen as an input for calculating the PT radiator (2.7). We have compared experimental values of $\langle x_Q \rangle$ extracted from leptonic c - and b -quark decays and $\langle x_{D^*} \rangle$ directly with the PT-motivated prediction for the quark energy losses.

Our treatment of the hadronization stage that implicitly appeals to duality arguments makes it plausible to apply a purely perturbative approach to inclusive quantities such as the lepton energy distributions. Meanwhile, it cannot pretend to describe *exclusive* heavy hadron spectra such as those of D^* , for example. Therefore, taking the measured mean energies of D^* for $\langle x_Q \rangle$ might introduce some systematic uncertainty to the fit, the error which is difficult to estimate.

Nonetheless, such a comparison has demonstrated that radiative charm and beauty losses may be consistently described in the energy range $W = 10 \rightarrow 90$ GeV within a variety of models for low-momentum behavior of the infrared-finite effective coupling α_s^{eff} . By tuning the shape parameter of a model, one achieves an accuracy of the common fit as good as $\chi^2/N_{\text{DF}} \approx 0.7/5$ (seven data points, two free parameters Λ and A/C).

We have checked that the fit to all data is consistent with the fits to high W , D^* , and inclusive lepton data samples.

At first sight, we have gained not much profit since we had to pay for eliminating an arbitrary non-PT fragmentation function by introducing another arbitrary function $\alpha_s^{\text{eff}}(k)$ at $k \lesssim 2$ GeV. An essential physically important difference between two approaches is that α_s^{eff} as a key ingredient of the PT-LPHD approach is supposed to be *universal* so that (quite substantial) differences between inclusive spectra of c - and b -flavored hadrons should be under control. By simultaneous fitting of the available experimental data on the energy losses in charm and beauty sectors, we have demonstrated consistency of the hypothesis of α_s^{eff} universality.

Moreover, the same notion of the infrared-finite effective coupling can be tried for a good many interesting problems in the light quark sector. An incomplete list of such phenomena for which the PT analysis has been carried out recently to next-to-leading order includes transverse [35] and longitudinal momentum distributions [36] in hadron-initiated processes, the energy-energy correlation [37], the thrust [38], and the heavy jet mass distribution [39] in e^+e^- annihilation.

The presence of the exponential of the characteristic integral over gluon momenta which emerges after all-order resummation of the Sudakov logarithms [40,41] is a common feature of the corresponding PT expres-

¹⁵A plausible rescaling procedure for extracting the non-PT part of the B meson fragmentation from the existing data on D meson spectra was suggested recently in [34].

sions. It is straightforward to derive quantitative PT-motivated predictions by implementing the universal α_s^{eff} in these integrals and, at the same time, by getting rid of non-PT “hadronization” effects which are usually taken into account by convoluting the PT distributions with phenomenological fragmentation functions (initial parton distributions for the case of hadron-initiated processes).

Carrying out this laborious but promising program, one should get valuable information about the confinement physics as seen through the eyes of the integrated influence of the large-distance hadron production upon inclusive particle distributions and/or event characteristics.

To this end the numerical results of our analysis of the heavy quark energy losses, namely,

$$(2 \text{ GeV})^{-1} \int_0^{2 \text{ GeV}} dk \frac{\alpha_s^{\text{eff}}(k)}{\pi} = 0.18 \pm 0.01(\text{expt}) \pm 0.02(\text{theor}), \quad (5.1a)$$

$$\alpha_{\overline{\text{MS}}}(M_Z) = 0.125 \pm 0.003(\text{expt}) \pm 0.004(\text{theor}), \quad (5.1b)$$

should be looked upon as a first hint for the more detailed study including the light quark phenomena discussed above.

One comment is in order concerning the nature of the results (5.1). The parallel description of c, b losses is sensitive to α_s^{eff} in the low-momentum range, say, of the order of (and below) M_b , so that the integral characteristic (5.1a) gets fixed quite sharply (theoretical error is due to our ignorance about the heavy quark masses and should be eliminated in the future).

At the same time such a description proves to be quite liberal to details of the high-momentum behavior of the coupling (one- versus two-loop α_s , number of active quark flavors). From this point of view, the value (5.1b) that one extracts at the end of the day is rather a tribute to (unfortunate) tradition. $\alpha_{\overline{\text{MS}}}(M_Z)$ should be looked upon as a reference value which emerges after theoretical extrapolation rather than a quantity that is “measured” by the above analysis. Theoretical error in (5.1b) is dominated by potential k^{-2} power correction effects in $\alpha_s^{\text{eff}}(k)$.

Let us stress again that in the low-momentum region behavior of the effective coupling is poorly known not because of the limited knowledge of higher order effects, but

rather because of an essentially different physical phenomenon that enters the game, the one that is usually referred to as confinement.

From this point of view, our notion of the infrared-finite α_s^{eff} differs from one that emerges from the three-loop analysis based upon the renormalization-scheme-invariant approaches to the e^+e^- annihilation cross section [42,43] and the τ -lepton hadronic width [42]. Nevertheless, it is worth mentioning that the value of the couplant $(\alpha_s/\pi)(0)$ and the integral measure obtained in [43] in the framework of the minimal sensitivity principle [44] are consistent with (5.1a).

Phenomenological verification of the fact that the effective QCD coupling stays numerically small would be of large practical value. Gribov theory of confinement [28] demonstrates how color confinement can be achieved in a field theory of light fermions interacting with comparatively small effective coupling, a fact of potentially great impact for enlarging the domain of applicability of perturbative ideology to the physics of hadrons and their interactions.

ACKNOWLEDGMENTS

We are indebted to V. N. Gribov and P. Mättig for many helpful discussions and valuable comments. One of us (Y.D.) is most grateful to the Theory Department of the University of Lund for the warm hospitality extended to him during the years when this study was being performed. This work was supported in part by the UK Particle Physics and Astronomy Research Council.

APPENDIX A: RUNNING COUPLING IN THE RADIATOR

1. Notation and kinematics

We consider production of a $Q\bar{Q}$ pair with on-mass-shell four-momenta p_1^μ, p_2^μ and a gluon with momentum k^μ by a colorless current with the total momentum q^μ . Hereafter, for a sake of simplicity we measure all the momenta and the quark mass in units of the total annihilation energy ($q^2 \equiv W^2 = 1$).

In terms of quark and gluon energy fractions,

$$z_i \equiv 2(p_i q), \quad z \equiv 2(k q), \quad z_1 + z_2 + z = 2;$$

$$2p_1 p_2 = (q - k)^2 - 2m^2 = 1 - z - 2m^2 + k^2 = z_1 + z_2 - 1 - 2m^2 + k^2, \quad (A1)$$

virtual quark propagators are

$$\kappa_1 \equiv (p_1 + k)^2 - m^2 = 1 - z_2, \quad \kappa_2 \equiv (p_2 + k)^2 - m^2 = 1 - z_1. \quad (A2)$$

[Relations (A2) do not imply $k^2 = 0$.]

Three-body kinematics restricts the difference of quark energy fractions as

$$4|\vec{k}|^2 \cdot \beta^2 \geq (z_1 - z_2)^2, \quad (\text{A3a})$$

where $\beta = \beta(z)$ represents the quark velocity in the rest frame of the $Q\bar{Q}$ pair ($Q\bar{Q}$ c.m.s.):

$$\beta^2 \equiv \frac{p_{Q\bar{Q}}^2}{E_{Q\bar{Q}}^2} = 1 - \frac{4m^2}{(p_1 + p_2)^2} = 1 - \frac{4m^2}{(q - k)^2}. \quad (\text{A3b})$$

a. $k^2 = 0$

For the on-mass-shell gluon case, one has $4|\vec{k}|^2 = z^2$, $(q - k)^2 = 1 - z$, and (A3) gives

$$\beta = \left(1 - \frac{4m^2}{1 - z}\right)^{1/2} \geq \left|\frac{z_1 - z_2}{z}\right|. \quad (\text{A4})$$

z, Θ_c basis. When the gluon energy is kept fixed, it is convenient to use the *scaled difference* of quark energies as a complementary variable related to the gluon angle in the $Q\bar{Q}$ c.m.s.:

$$u \equiv \frac{z_1 - z_2}{z} = \frac{2(p_1 - p_2)k}{2(p_1 + p_2)k} = \beta \cos \Theta_c, \quad -\beta \leq u \leq +\beta. \quad (\text{A5})$$

The maximal value $|u| = \beta$ is reached when the gluon is *collinear* with one of the quarks.

Introducing the maximal quark velocity v ,

$$\beta^2 \leq v^2 \equiv 1 - 4m^2 \geq z, \quad (\text{A6})$$

one may present the integration phase space as

$$\int dz_1 \int dz_2 = \frac{1}{2} \int_0^{v^2} z dz \int_{-\beta}^{\beta} du. \quad (\text{A7})$$

Some useful relations are

$$1 - u^2 = 4(1 - z_1)(1 - z_2)z^{-2}, \quad (\text{A8a})$$

$$\begin{aligned} \left(\frac{1 - z_1}{1 - z_2} + \frac{1 - z_2}{1 - z_1}\right) &= \frac{z^2}{(1 - z_1)(1 - z_2)} - 2 \\ &= \frac{4}{1 - u^2} - 2. \end{aligned} \quad (\text{A8b})$$

x, y basis. For the purpose of deriving a single-inclusive-quark spectrum, we break the symmetry between z_1, z_2 and denote

$$x \equiv z_1, \quad y \equiv 1 - z_2.$$

One has to fix x and integrate over y in the limits $y_- \leq y \leq y_+$, which follow from the kinematical restriction (A4). In terms of x, y the latter takes the form

$$y^2(1 - z + m^2) - y(x - 2m^2)(1 - x) + m^2(1 - x)^2 \leq 0. \quad (\text{A9})$$

This gives

$$y_{\pm} = \frac{1 - x}{2(1 - x + m^2)}(x - 2m^2 \pm \sqrt{x^2 - 4m^2}).$$

Introducing

$$z_0 \equiv \frac{1}{2}(x - 2m^2 + \sqrt{x^2 - 4m^2}) = x + O(m^2), \quad (\text{A10})$$

one may write [cf. (2.8)]

$$y_+ = \frac{(1 - x)z_0}{1 - x + m^2} = x[1 + O(m^2)], \quad (\text{A11})$$

$$y_- = \frac{1 - x}{z_0} m^2 = \frac{1 - x}{x} m^2 [1 + O(m^2)].$$

Useful relations are

$$y_+ - y_- = \frac{1 - x}{1 - x + m^2} \sqrt{x^2 - 4m^2}, \quad (\text{A12a})$$

$$(y_-)^{-1} - (y_+)^{-1} = \frac{\sqrt{x^2 - 4m^2}}{1 - x} m^{-2}, \quad (\text{A12b})$$

$$(y_+)^2 - (y_-)^2 = (x - 2m^2) \sqrt{x^2 - 4m^2} \left(\frac{1 - x}{1 - x + m^2}\right)^2. \quad (\text{A12c})$$

b. $k^2 > 0$

If we allow the gluon to have a positive virtuality k^2 , (A3) takes the form

$$(z_1 - z_2)^2 \leq (z^2 - 4k^2) \left(1 - \frac{4m^2}{1 - z + k^2}\right) \quad (\text{A13})$$

and leads to the following maximal invariant gluon mass for given z_1, z_2 :

$$\begin{aligned} k^2 \leq k_m^2 &= (1 - z_1)(1 - z_2) - \frac{1}{2}[z_1 z_2 - 4m^2 - \sqrt{z_1 - 4m^2} \sqrt{z_2 - 4m^2}] \\ &= \left\{ \frac{2(1 - x + m^2)}{x - (2 - x)y - 4m^2 + \sqrt{x^2 - 4m^2}[(1 - y)^2 - 4m^2]} \right\} (y_+ - y)(y - y_-). \end{aligned} \quad (\text{A14})$$

As we shall see below, the structure of the matrix element is such that essential contributions emerge from the logarithmic region $y_- \ll y \ll y_+$, as well as from the vicinity of the *lower* limit, $(y-y_-) \sim y_- \sim m^2$. Therefore for our purposes the following approximate expression suffices:

$$k_m^2 = (1-x)(y-y_-) + O(m^2), \quad (\text{A15})$$

which differs from the exact formula (A14) only in a tiny region close to the *upper* integration limit, $(y_+-y) \sim m^2$.

Two characteristic momentum scales emerge related to the limiting values of the y integration [cf. (2.8)]:

$$Q^2(x) \equiv W^2(1-x)y_+ \approx W^2x(1-x), \quad (\text{A16})$$

$$\kappa^2(x) \equiv W^2(1-x)y_- \approx M^2(1-x)^2/x.$$

2. VASP cross sections

The differential first order cross section integrated over angles of the final $Q\bar{Q}g$ system may be written as

$$\left\{ \frac{d^2\sigma_{Q\bar{Q}g}}{dz_1 dz_2} \right\}_C = \sigma^\infty \frac{C_F \alpha_s}{2\pi} \Pi_C. \quad (\text{A17})$$

The subscript C marks the production current [vector (V), axial vector (A), scalar (S), or pseudoscalar (P)] and $\sigma^{(\infty)}$ is the universal high-energy limit of the Born transition probability, current (C) $\rightarrow Q\bar{Q}$.

A straightforward calculation leads to the following expression for the Π factors:¹⁶

$$\Pi_C = 2\zeta_C \mathcal{S} + \mathcal{H}_C, \quad (\text{A18a})$$

$$\mathcal{H}_V = \left(\frac{1-z_1}{1-z_2} + \frac{1-z_2}{1-z_1} \right) = (1-z) \frac{1}{y} + \frac{y}{1-x}, \quad (\text{A18b})$$

$$\mathcal{H}_A = (1+2m^2)\mathcal{H}_V + 4m^2, \quad \mathcal{H}_S = \mathcal{H}_P = \mathcal{H}_V + 2. \quad (\text{A18c})$$

Here \mathcal{S} is the "soft" bremsstrahlung term:

$$\begin{aligned} \mathcal{S} &\equiv - \left(\frac{p_{1\mu}}{\kappa_1} - \frac{p_{2\mu}}{\kappa_2} \right)^2 = \frac{z_1 + z_2 - 1 - 2m^2}{(1-z_1)(1-z_2)} - \frac{m^2}{(1-z_1)^2} - \frac{m^2}{(1-z_2)^2} \\ &= \frac{x - 2m^2}{1-x} \frac{1}{y} - \frac{m^2}{y^2} - \frac{1-x+m^2}{(1-x)^2}. \end{aligned} \quad (\text{A19})$$

Its contribution to each of the squared matrix elements is explicitly proportional to corresponding ζ factor, the one that determines the energy dependence of the corresponding $Q\bar{Q}$ Born cross section:

$$\sigma_{Q\bar{Q}} = \sigma^\infty v \zeta_C(v); \quad (\text{A20a})$$

$$\zeta_V = \frac{3-v^2}{2} = 1 + 2m^2, \quad (\text{A20b})$$

$$\zeta_A = \zeta_S = v^2 = 1 - 4m^2, \quad \zeta_P = 1.$$

As a result, the *normalized* differential distribution can be written in the following general form as a sum of a *universal* "soft" and a process-dependent "hard" contribution:

$$d^2w_C \equiv \left\{ \frac{d^2\sigma_{Q\bar{Q}g}}{\sigma_{Q\bar{Q}}} \right\}_C = \frac{C_F \alpha_s}{2\pi v} \{ 2\mathcal{S} + \zeta_C^{-1} \mathcal{H}_C \} dx dy. \quad (\text{A21})$$

z, Θ_c basis. Both the structure of the matrix element and the kinematics become particularly simple in terms of the gluon energy fraction and gluon angle in the $Q\bar{Q}$ c.m.s. [see (A5)]. Making use of (A8), one gets

$$\mathcal{S} = \frac{4(1-z)}{z^2} \frac{\beta^2 - u^2}{(1-u^2)^2} = \frac{4(1-x)}{z^2} \frac{\beta^2 \sin^2 \Theta_c}{(1-\beta^2 \cos^2 \Theta_c)^2} \frac{4m^2}{1-z+4m^2}, \quad (\text{A22a})$$

$$\mathcal{H}_V = \frac{4}{1-u^2} - 2 = \frac{4}{1-\beta^2 \cos^2 \Theta_c} - 2. \quad (\text{A22b})$$

¹⁶See [24] for details.

Invoking (A7), (A21), we obtain, for the inclusive gluon energy spectrum in the vector channel (see also [45]),

$$dw_V = \frac{C_F \alpha_s}{\pi} \frac{dz}{z} \frac{\beta}{v} \int_{-1}^1 d \cos \Theta_c \left\{ 2(1-z) \frac{\beta^2 \sin^2 \Theta_c}{(1-\beta^2 \cos^2 \Theta_c)^2} + z^2 \left[\frac{1}{1-\beta^2 \cos^2 \Theta_c} - \frac{1}{2} \right] \zeta_V^{-1} \right\}. \quad (\text{A23})$$

Our convention to call the two pieces of the matrix element “soft” and “hard” becomes clear now: In the soft gluon limit $z \ll 1$, the second term is z^2 down compared to the first one. In this representation the “dead cone” phenomenon is also manifesting: The soft *classical* term \mathcal{S} vanishes in the very forward directions ($\Theta_c, \pi - \Theta_c < \theta_0 = m$).

In a relativistic situation ($m \ll \frac{1}{2}$), a collinear logarithmic enhancement occurs and the two pieces of (A23) participate in forming the GLAP-splitting function:

$$dw \propto \frac{d\Theta_c^2}{\Theta_c^2} \{2(1-z) + z^2\} \frac{dz}{z} \propto \frac{1+(1-z)^2}{z} dz.$$

It is worthwhile to notice that the $O(z^{-1})$ and $O(1)$ parts of the $q \rightarrow q+g(z)$ splitting function are process independent, while the $O(z)$ piece breaks factorization at the level of the $O(m^2 \ln m^2)$ correction. Therefore the very notion of “fragmentation function” as a way of treating the jet evolution independently of the production mechanism gets lost beyond the leading twist.

To stress the logarithmic character of the angular integration, one may represent (A23) as

$$dw_V = \frac{C_F \alpha_s}{\pi v} \frac{dz}{z} \int_{\eta_0}^1 \frac{d\eta}{\sqrt{1-\eta}} \left\{ 2(1-z) \frac{\eta - \eta_0}{\eta^2} + z^2 \left[\frac{1}{\eta} - \frac{1}{2} \right] \zeta_V^{-1} \right\}, \quad (\text{A24a})$$

where

$$\eta \equiv 1 - u^2 = 1 - \beta^2 \cos^2 \Theta_c \geq \eta_0 \equiv \frac{4m^2}{1-z}. \quad (\text{A24b})$$

For other production channels, the second “hard” term in (A23), (A24a) should be changed according to (A18c), (A20b).

3. Integration over virtual boson mass

Considering *inclusive* characteristics (e.g., such as the quark energy spectrum) beyond first order of perturbation theory, one has to allow the gluon to decay in the final state, that is, to have a positive virtuality k^2 , and to integrate over the latter within the available phase space. Actually, only such a combination of real and virtual gluon production leads to a sensible physical answer. First of all, an *exclusive* real gluon production cross section is clearly zero because of the standard infinite (double logarithmic) Sudakov form factor suppression. Second, and more importantly, a “real” gluon is an ill-defined object since its “on-mass-shell” interaction strength α_0 may not be defined perturbatively (which is a *real* “infrared catastrophe” inherent in QCD).

Integration over k^2 leads to the appearance of the running coupling in the inclusive cross section. This nice property, discovered in the pioneering papers by Gribov and Lipatov on the partonic structure of logarithmic field theories [17], is particularly helpful in the QCD context. Here neither α_0 in “elastic” radiation nor small virtuality inelastic gluon decay systems are well defined. Meanwhile, their combined action results in a legitimate $\alpha_s(k_m)$ at the Euclidean scale related to the maximal

available gluon virtuality.

We shall demonstrate this correspondence, taking care of subleading effects which might be relevant within the adopted approximation. To this end we write down a formal dispersion relation (with one subtraction) for the running coupling:

$$\alpha(Q^2) \equiv \alpha_0 \mathcal{Z}_3(-Q^2) = \alpha_0 + Q^2 \int_0^\infty \frac{dk^2}{k^2} \frac{\sigma(k^2)}{k^2 + Q^2}, \quad (\text{A25a})$$

where σ is related to discontinuity of \mathcal{Z}_3 at positive virtuality,

$$\begin{aligned} \sigma(k^2) &\equiv \frac{\alpha_0}{2\pi i} [\mathcal{Z}_3(k^2 - i\epsilon) - \mathcal{Z}_3(k^2 + i\epsilon)] \\ &\equiv -\frac{\alpha_0}{2\pi} \text{Disc}\{\mathcal{Z}_3(k^2)\}. \end{aligned} \quad (\text{A25b})$$

In QED, \mathcal{Z}_3 is nothing but the photon renormalization function and $\alpha_0 \approx \frac{1}{137}$ is the on-mass-shell coupling constant.

Strictly speaking, such an identification is true for an Abelian theory only. In the QCD context the Ward identity between vertex and fermion propagator corrections, $\mathcal{Z}_\Gamma \mathcal{Z}_q = 1$, does not hold. As is well known, both the non-Abelian vertex renormalization correction $\mathcal{Z}_\Gamma^{(\text{NA})}$ and the gluon propagator factor \mathcal{Z}_g participate (in a gauge-dependent way) in forming the running α_s . So one has to look upon \mathcal{Z}_3 in the dispersion relation (A25) as the gauge-invariant product

$$\mathcal{Z}_3 = \mathcal{Z}_\Gamma^{(\text{NA})} \mathcal{Z}_g \mathcal{Z}_\Gamma^{(\text{NA})}.$$

This subtlety does not affect the result, however.

Another motivation is to use the n_f dependence as a gauge to pinpoint the structure of the running α_s in the inclusive cross section [22]. Quark loops (in order

α^2) belong to \mathcal{Z}_g only, and employing a “quasi-Abelian” relation (A25) becomes natural.

In the problem under consideration, the following structure emerges:

$$\begin{aligned} \alpha_0 M(z_1, z_2; 0) + \int_0^{k_m^2} \frac{dk^2}{k^2} \sigma(k^2) M(z_1, z_2; k^2) \\ = \left\{ \alpha_0 + \int_0^{k_m^2} \frac{dk^2}{k^2} \sigma(k^2) \right\} M(z_1, z_2; 0) + \int_0^{k_m^2} dk^2 \sigma(k^2) \Delta M(z_1, z_2; k^2), \end{aligned} \quad (\text{A26})$$

with $k_m^2 = k_m^2(z_1, z_2)$ the maximal squared virtual boson mass allowed for given x, y . Here we have singled out the $k^2 = 0$ part of the matrix element by writing

$$M(z_1, z_2; k^2) = M(z_1, z_2; 0) + k^2 \Delta M(z_1, z_2; k^2). \quad (\text{A27})$$

Now we may relate the characteristic integral in the first term in the right-hand side (RHS) of (A26) with the dispersion formula (A25a). To this end we employ the following *exact* representation of the dispersion relation:

$$\alpha(Q^2) = \alpha_0 + Q^2 \int_0^\infty \frac{dk^2 \sigma(k^2)}{k^2(k^2 + Q^2)} = \alpha_0 + \int_0^{Q^2} \frac{dk^2}{k^2} \sigma(k^2) + \int_0^1 \frac{dt}{1+t} [\sigma(Q^2/t) - \sigma(Q^2 t)]. \quad (\text{A28})$$

Perturbatively, σ is of the order of α^2 . As a result, the last finite integral term constitutes a *next-to-next-to-leading* correction to the main one. To see this one has to view σ as a slowly varying (logarithmic) function of its argument¹⁷ and to perform the Taylor expansion in $\ln Q^2$ to obtain

$$\int_0^1 \frac{dt}{1+t} [\sigma(Q^2/t) - \sigma(Q^2 t)] = -2\sigma'(Q^2) \int_0^1 \frac{dt}{1+t} \ln t + O(\sigma''') \approx \frac{\pi^2}{6} \sigma'(Q^2).$$

This exercise demonstrates a close correspondence between the spectral density (A25b) and the β function [46]:

$$\alpha(Q^2) = \alpha_0 + \int_0^{Q^2} \frac{dk^2}{k^2} \sigma(k^2) + \frac{\pi^2}{6} \sigma'(Q^2) + \dots, \quad (\text{A29a})$$

$$\sigma(Q^2) = \alpha'(Q^2) - \frac{\pi^2}{6} \alpha'''(Q^2) + O(\alpha^{(V)}). \quad (\text{A29b})$$

Thus we express perturbatively the structure in the curly brackets in (A26) in terms of the running coupling at the Euclidean point $Q^2 = k_m^2$:

$$\bar{\alpha}(k_m^2) \equiv \left\{ \alpha_0 + \int_0^{k_m^2} \frac{dk^2}{k^2} \sigma(k^2) \right\} = \alpha(k_m^2) - \frac{\pi^2}{6} \alpha''(k_m^2) + \dots. \quad (\text{A30})$$

4. Running coupling in the first order spectrum

It is straightforward to calculate the exact $Q\bar{Q}g$ matrix element with account of a nonzero virtual gluon mass $k^2 > 0$. Equation (A21) gets modified as follows:

$$2S \Rightarrow 2S^{(0)} - k^2 \left(\frac{1}{(1-z_1)^2} + \frac{1}{(1-z_2)^2} \right), \quad (\text{A31a})$$

$$\mathcal{H}_V \Rightarrow \mathcal{H}_V^{(0)} + 2k^2 \frac{z_1 + z_2 + k^2}{(1-z_1)(1-z_2)}, \quad (\text{A31b})$$

where $S^{(0)}$ and $\mathcal{H}_V^{(0)}$ are given by the original “on-mass-shell-boson” expressions (A19) and (A18b), respectively. In terms of (A27),

$$\Delta\{2S\} = -\frac{1}{y^2} - \frac{1}{(1-x)^2}, \quad (\text{A32a})$$

¹⁷Which is true everywhere except in the very vicinity of a fermion threshold.

$$\Delta\{\mathcal{H}_V\} = \frac{2(1+x-y+k^2)}{(1-x)y}. \quad (\text{A32b})$$

a. $k^2 = 0$ part of the matrix element

To evaluate the radiator (2.7), we start by considering the first term in (A26) proportional to $M(z_1, z_2; 0)$. One has to perform the y integration with the factor $\tilde{\alpha}$ that emerges after integration over virtual boson mass [see (A30)],

$$\int_{y_-}^{y_+} dy \tilde{\alpha}(k_m^2(x, y)) \{2S^{(0)} + \zeta_V^{-1} \mathcal{H}^{(0)}\}, \quad (\text{A33})$$

with k_m^2 given by the approximate expression (A15). Invoking (A19), (A18b), we split the integrand into three pieces as follows:

$$\{2S^{(0)} + \zeta_V^{-1} \mathcal{H}^{(0)}\} = \left\{ 2 \frac{x-2m^2}{1-x} + \zeta_V^{-1} (1-x) \right\} \frac{1}{y} \quad (\text{A34a})$$

$$-2 \frac{m^2}{y^2} \quad (\text{A34b})$$

$$-2 \frac{1-x+m^2}{(1-x)^2} + \zeta_V^{-1} \frac{y}{1-x}. \quad (\text{A34c})$$

Logarithmic piece (A34a). This is the leading contribution to the radiator, in which the y integration is logarithmic (collinear logarithm):

$$\int_{y_-}^{y_+} \frac{dy}{y} \tilde{\alpha}(y-y_-). \quad (\text{A35})$$

Here we have explicitly shown the essential y dependence of the coupling factor $\tilde{\alpha}$. The chain of approximations follows:

$$\begin{aligned} (\text{A35}) &= \int_{y_-}^{y_+} \frac{dy}{y} \left(\tilde{\alpha}(y) + \tilde{\alpha}'(y) \ln \frac{y-y_-}{y} + \dots \right) \approx \int_{y_-}^{y_+} \frac{dy}{y} \tilde{\alpha}(y) + \tilde{\alpha}'(y) \int_{y_-/y_+}^1 \frac{ds}{s} \ln(1-s) \\ &\approx \int_{y_-}^{y_+} \frac{dy}{y} \tilde{\alpha}(y) - \frac{\pi^2}{6} \tilde{\alpha}'(y_-) = \int_{\kappa^2}^{\mathcal{Q}^2} \frac{dt}{t} \alpha(t) - \frac{\pi^2}{6} \alpha'(\mathcal{Q}^2) + O(\alpha^3(\kappa^2) + \alpha^3(\mathcal{Q}^2)), \end{aligned} \quad (\text{A36})$$

where (A30) has been used. We notice that a potential second order contribution $\alpha' \propto \alpha^2$ at the low scale $\kappa^2 \sim M^2$ cancels out, and the remaining term $\alpha'(\mathcal{Q}^2) \propto \alpha^2(W^2)$ is comparable with the two-loop correction to the hard cross section (coefficient function) and must be neglected within our approximation.

Finally,

$$\int dy (\text{A34a}) = \left(2 \frac{x-2m^2}{1-x} + \zeta_V^{-1} (1-x) \right) \int_{\kappa^2}^{\mathcal{Q}^2} \frac{dt}{t} \alpha(t). \quad (\text{A37})$$

Singular piece (A34b). The second term of (A34) originates from the dead cone subtraction. It is explicitly proportional to m^2 , but this suppression gets compensated by the singular behavior in y . The corresponding y integral is concentrated in a tiny region $(y-y_-) \sim y_- \propto m^2$:

$$\int_{y_-}^{y_+} \frac{dy}{y^2} \tilde{\alpha}(y-y_-) = \alpha(y_-) \int_{y_-}^{y_+} \frac{dy}{y^2} \alpha'(y_-) \int_{y_-}^{y_+} \frac{dy}{y^2} \ln \frac{y-y_-}{y_-} + O(\alpha''(y_-)). \quad (\text{A38})$$

The $O(\alpha^2(y_-))$ term vanishes in the relativistic approximation:

$$\int_{y_-}^{y_+} \frac{dy}{y^2} \ln \frac{y-y_-}{y_-} = \int_0^{(y_+-y_-)/y_-} \frac{ds}{(1+s)^2} \ln s \approx \int_0^\infty \frac{ds}{(1+s)^2} \ln s = 0.$$

Thus, similarly to what has happened to the logarithmic term (A34a) discussed above, a potential $O(\alpha^2(\kappa))$ contribution is absent. One is left with a pure $\alpha(\kappa^2)$ correction to the radiator:

$$\int dy (\text{A34b}) = -2m^2 \left\{ \frac{1}{y_-} - \frac{1}{y_+} \right\} \alpha(\kappa^2) = -2 \frac{\sqrt{x^2-4m^2}}{1-x} \alpha(\kappa^2). \quad (\text{A39})$$

Finite piece (A34c). The corresponding y integral is collinear safe (i.e., finite in the $m^2 = 0$ limit) and constitutes an $\alpha(W^2)$ correction to the hard cross section. Here one extracts the coupling at the upper limit, $y \sim y_+$, and the y integration becomes trivial [see (A12)]:

$$\begin{aligned} \int dy(A34c) &= \alpha(Q^2) \left\{ -2 \frac{(1-x+m^2)(y_+ - y_-)}{(1-x)^2} + \zeta_V^{-1} \frac{\frac{1}{2}(y_+^2 - y_-^2)}{1-x} \right\} [1 + O(\alpha(Q^2))] \\ &\approx \alpha(Q^2) \sqrt{x^2 - 4m^2} \left\{ -\frac{2}{1-x} + \zeta_V^{-1} \frac{x - 2m^2}{2(1-x)} \left(\frac{1-x}{1-x+m^2} \right)^2 \right\}. \end{aligned} \quad (A40)$$

b. Δ part of the matrix element

At first sight, the corrections (A32) to the $Q\bar{Q}g$ matrix element proportional to virtual boson mass look negligible: The corresponding k^2 integration is no longer logarithmic, $k^2 \sim k_m^2$, and the result is of the order of $\sigma(k_m^2) \propto \alpha^2(k_m^2)$.

This expectation indeed comes true for the “hard” correction term (A32b) as well as for the second piece of (A32a). However, the first contribution to the “soft” correction term (A32a) is *oversingular* in y , as a result of which singularity logarithmic behavior gets restored and a contribution to the two-loop anomalous dimension emerges.

Indeed,

$$\int_0^{k_m^2} dk^2 \sigma(k^2) = k_m^2 \left\{ \sigma(k_m^2) + \sigma'(k_m^2) \int_0^{k_m^2} \frac{dk^2}{k_m^2} \ln \frac{k^2}{k_m^2} + \dots \right\} \equiv k_m^2 \tilde{\sigma}(k_m^2), \quad (A41a)$$

where

$$\tilde{\sigma} = \alpha' - \alpha'' + O(\alpha'''). \quad (A41b)$$

Invoking (A15) for k_m^2 , one arrives at the following expression for the Δ correction:

$$-(1-x) \int_{y_-}^{y_+} \frac{dy}{y^2} (y - y_-) \tilde{\sigma}(y - y_-). \quad (A42)$$

An approximate evaluation follows:

$$\begin{aligned} \int_{y_-}^{y_+} \frac{dy}{y^2} (y - y_-) \tilde{\sigma}(y - y_-) &= \int_{y_-}^{y_+} \frac{dy}{y^2} (y - y_-) \tilde{\sigma}(y) O(\tilde{\sigma}'(y_-)) \\ &\approx \int_{y_-}^{y_+} \frac{dy}{y} \tilde{\sigma}(y) - \tilde{\sigma}(y_-) = [\alpha(Q^2) - \alpha(\kappa^2) - \alpha'(Q^2) + \alpha'(\kappa^2)] - [\alpha'(\kappa^2) + \dots]. \end{aligned} \quad (A43)$$

Again, as before, the $\alpha^2(\kappa^2)$ contribution cancels, and one finally gets the correction

$$\int dy \int dk^2 \sigma(k^2) \Delta M(x, y; k^2) = -(1-x) [\alpha(Q^2) - \alpha(\kappa^2)] + O(\alpha^2(Q^2) + \alpha^3(\kappa^2)). \quad (A44)$$

Combining (A37), (A39), (A40), and (A44), we finally arrive at expression (2.7) for the perturbative radiator.

APPENDIX B: SECOND LOOP ANOMALOUS DIMENSION $\Delta^{(2)}$

1. AD (dimensional regularization)

The two-loop anomalous dimension (AD) has been derived in the framework of a dimensional regularization approach in [18–20]. In the notation of Curci, Furmanski, and Petronzio [18], the nonsinglet AD corresponding to $Q \rightarrow Q$ transition in *spacelike* evolution reads [Eqs. (4.50)–(4.54) of [18]]

$$C_F^{-1} \hat{P}_{qq}(x, a) = aP(x) + a^2 \gamma^{(2)}(x), \quad P(x) \equiv \frac{1+x^2}{1-x}, \quad (B1)$$

where

$$\gamma^{(2)} = C_F P_F(x) + C_A P_G(x) + n_f T_R P_{n_f}(x),$$

$$P_F = -2P(x) \ln x \ln(1-x) - \left(\frac{3}{1-x} + 2x \right) \ln x - \frac{1}{2} (1+x) \ln^2 x - 5(1-x), \quad (B2a)$$

$$P_G = P(x) \left[\frac{1}{2} \ln^2 x + \frac{11}{6} \ln x + \frac{67}{18} - \frac{\pi^2}{6} \right] + (1+x) \ln x + \frac{20}{3}(1-x), \quad (\text{B2b})$$

$$P_{n_f} = -\frac{2}{3} \left[P(x) \left(\ln x + \frac{5}{3} \right) + 2(1-x) \right]. \quad (\text{B2c})$$

Let us mention an extra contribution due to the $Q \rightarrow \bar{Q} + QQ$ transition which reads

$$C_F^{-1} \hat{P}_{q\bar{q}}(x, a) = a^2 (C_F - \frac{1}{2} C_A) \{ 2P(-z) S_2(x) + 2(1+x) \ln x + 4(1-x) \}, \quad (\text{B3a})$$

with

$$S_2(x) \equiv \int_{x(1+x)^{-1}}^{(1+x)^{-1}} \frac{dz}{z} \ln \frac{1-z}{z}. \quad (\text{B3b})$$

This contribution (which formally belongs to the *nonsinglet* AD; see, e.g., [15]) vanishes as $(1-x)^2$ at large x and is color suppressed and numerically negligible. In this paper it has been disregarded together with the *singlet* (sea) contribution to heavy quark yield.

An algebraic massage leads to the following representation for the quark evolution kernel:¹⁸

$$C_F^{-1} \hat{P}_{qq}(x, a) = [a + \mathcal{K}a^2] P(x) + a^2 \{ \sigma C_F \mathcal{V}(x) + \mathcal{R}(x) \} - a' [P(x) \ln x + 2(1-x)]. \quad (\text{B4})$$

The first term here collects the one-loop AD with the part of $\gamma^{(2)}$ correction explicitly proportional to $P(x)$ with the number \mathcal{K} given by (2.16b) above. These two combine forming a “physical” coupling in terms of the $\overline{\text{MS}}$ one according to (2.17b). This term totally absorbs the $(1-x)^{-1}$ singularity of the evolution kernel: $\mathcal{V}(x) \propto \ln(1-x)$, and $\mathcal{R}(x)$ vanishes as $(1-x)$ in the quasielastic limit. [The very last term in (B4) proportional to the derivative of the running coupling,

$$a' \equiv \frac{d}{d \ln W^2} \frac{\alpha_s(Q)}{2\pi} = -\left(\frac{11}{6} N_c - \frac{2}{3} T_R n_f \right) a^2 + \dots, \quad (\text{B5})$$

does not count, as it is an artifact of the dimensional regularization scheme; see below.]

The “true” second loop AD in curly brackets of (B4) consists of two contributions. The first one is

$$\begin{aligned} \mathcal{V}(x) &= - \left[P(x) \left(\ln \frac{x}{(1-x)^2} - \frac{3}{2} \right) + (1-x) - \frac{1}{2}(1+x) \ln x \right] \ln x \\ &= \int_0^1 dz \int_0^1 dy \delta(x-yz) \{ P(y) \}_+ P(z) \ln(z). \end{aligned} \quad (\text{B6a})$$

So defined, \mathcal{V} has a very simple form in the moment representation; namely,

$$\mathcal{V}(j) \equiv \int_0^1 dx x^{j-1} \mathcal{V}(x) = P_j \frac{d}{dj} P_j \left(P_j \equiv \int_0^1 dx P(x)_+ = \int_0^1 dx [x^{j-1} - 1] \frac{1+x^2}{1-x} \right). \quad (\text{B6b})$$

(Obviously, $[\mathcal{V}(x)]_+ = \mathcal{V}(x)$.) This (and only this) contribution changes (acquires an opposite sign) when timelike evolution is considered [18]. Therefore (B4) holds for both channels with $\sigma = \pm 1$ referring to timelike and spacelike evolution correspondingly. The origin of the \mathcal{V} term in the two-loop kernel may be traced back to a simple kinematical difference between annihilation and scattering channels [18]. It has been argued [47] that a mismatch between the two-loop e^+e^- and deep inelastic scattering (DIS) anomalous dimensions would disappear (and thus the Gribov-Lipatov relation [17] would be rescued) if one considered scaling violation of “pseudomoments” in x evaluated for a fixed value of $\{xW^2\}_{\text{annih}} = \{Q^2/x\}_{\text{scatt}}$.

Another term of the second loop AD is

$$\mathcal{R}(x) = \left(\frac{1}{2} C_A - C_F \right) P(x) \ln^2 x - 5C_F \left[\frac{1}{2}(1+x) \ln x + (1-x) \right] + C_A \{ (1+x) \ln x + 3(1-x) \}. \quad (\text{B7})$$

Similarly to the one-loop splitting function $P(x)$, it obeys the reciprocity relation [17]

¹⁸The “+” prescription is implicit.

$$-x\mathcal{R}(x^{-1}) = \mathcal{R}(x) \quad (\text{B8a})$$

and, as a result, stays the same for timelike and spacelike evolution. Contrary to this,

$$-x\mathcal{V}(x^{-1}) = [-1]\mathcal{V}(x). \quad (\text{B8b})$$

2. CF (dimensional regularization)

The $O(a)$ correction to the hard cross section [18,19] [coefficient function (CF)] has to be taken into consideration together with the two-loop AD since neither the CF nor AD is a scheme-independent quantity beyond leading logarithms.

It reads [see Eqs. (7.4), (7.10) of [18]]

$$C_2^A = \delta(1-x) + aC_F \left\{ \left[\frac{1+x^2}{1-x} \left(\ln \frac{1-x}{x} - \frac{3}{4} \right) + \frac{1}{4}(9+5x) \right]_+ + \frac{3(1+x)^2}{1-x} \ln x - \frac{7}{2}(1+x) + \pi^2 \delta(1-x) \right\}, \quad (\text{B9a})$$

$$C_L^A = aC_F. \quad (\text{B9b})$$

The first line of (B9a) is the CF for the scattering channel (C_2^S); the second line accounts for their difference. After simple manipulations one arrives at

$$C_2^A = (1 - \frac{3}{2}aC_F)\delta(1-x) + aC_F [P(x)\{\ln[x^2(1-x)] - \frac{3}{4}\} - \frac{1}{4}(5+9x)]_+. \quad (\text{B10})$$

In the cross section integrated over the total $Q\bar{Q}g$ production angle [see (2.3)], the combination $C_2^A + 3C_L^A$ emerges. With account of the longitudinal contribution, the $\delta(1-x)$ term gets modified:

$$C^A(x, a) \equiv C_2^A + 3C_L^A = (1 - \frac{3}{2}aC_F)\delta(1-x) + aC_F[(\text{B10})]_+ + 3aC_F \\ = (1 + \frac{3}{2}aC_F)\delta(1-x) + aC_F[(\text{B10}) + 3]_+. \quad (\text{B11})$$

Constructing the CF that describes quark distribution *normalized* by the total cross section,

$$C_i(x, a) = (1 + \frac{3}{2}aC_F)^{-1} C^A(x, a), \quad (\text{B12})$$

one gets, with $O(a)$ accuracy, the answer, which may be presented in the form

$$C_i(x, a) = \delta(1-x) + aC_F [P(x)\{\ln[x(1-x)] - \frac{3}{4}\} - \frac{1}{4}(1+x)]_+ + aC_F \{P(x) \ln x + 2(1-x)\}_+. \quad (\text{B13})$$

3. Scaling violation rate

The scaling violation rate is an observable determined by the scheme-invariant combination

$$D' \equiv \frac{d}{d \ln W^2} D(x, W^2) \implies \hat{P}_{qq}(x, a(W^2)) + \frac{d}{d \ln W^2} C_i(x, a(W^2)). \quad (\text{B14})$$

Combining (B4) and (B13), one arrives at¹⁹

$$D' \implies [a_{\overline{\text{MS}}} + \mathcal{K}a^2] C_F P(x) + a^2 C_F \{C_F \mathcal{V}(x) + \mathcal{R}(x)\} + a' C_F [P(x)\{\ln[x(1-x)] - \frac{3}{4}\} - \frac{1}{4}(1+x)], \quad (\text{B15})$$

where the $\overline{\text{MS}}$ origin of the running coupling has been stressed in the relevant first order term.

This result has to be compared with the scaling violation rate as described by (2.7). To this end one evaluates the $\ln W^2$ derivative of the relativistic radiator (2.10) to obtain

¹⁹The "+" prescription is implicit.

$$D' \Rightarrow \{a(Q^2)C_F P(x) - a' C_F(1-x) + a^2 C_F \Delta^{(2)}\} + a' C_F \left\{ \frac{-2x}{1-x} + \frac{x^2}{2(1-x)} \right\}. \quad (\text{B16})$$

In the leading term one has to expand the coupling of a composite argument Q^2 near W^2 as

$$a(Q^2) = a(W^2) + a' \ln[x(1-x)] + \dots. \quad (\text{B17})$$

Adding together terms proportional to a' , one observes a correspondence with a relevant part of (B15):

$$-\frac{2x}{1-x} = -P(x) + (1-x), \quad \frac{x^2}{2(1-x)} = \frac{1}{4}P(x) - \frac{1}{4}(1+x),$$

$$\ln[x(1-x)] - (1-x) - \frac{2x}{1-x} + \frac{x^2}{2(1-x)} = P(x) \left\{ \ln[x(1-x)] - \frac{3}{4} \right\} - \frac{1}{4}(1+x).$$

Identifying

$$(\text{B15}) = (\text{B16}), \quad (\text{B18})$$

we arrive at the final result, which relates an “effective” (dispersion scheme motivated) coupling a_{eff} with $a_{\overline{\text{MS}}}$ and gives an expression for the “true” second loop correction to the radiator $\tilde{\Delta}^{(2)}$ we were aiming at

$$a_{\text{eff}} C_F P(x) + a^2 C_F \tilde{\Delta}^{(2)} = [a_{\overline{\text{MS}}} + \mathcal{K} a^2] C_F P(x) + a^2 C_F \{C_F \mathcal{V}(x) + \mathcal{R}(x)\}. \quad (\text{B19})$$

-
- [1] For reviews, see, e.g., P. Mättig, in *Proceedings of the 4th International Symposium on Heavy Flavor Physics*, Orsay France, 1991, edited by M. Davier and G. Wormser (Editions Frontières, Gif-sur-Yvette, 1991); T. Behnke, in *Proceedings of the 26th International Conference on High Energy Physics*, Dallas, Texas, 1992, edited by J. R. Sanford, AIP Conf. Proc. No. 272 (AIP, New York, 1993), Vol. I, p. 859; see also *QCD 94*, Proceedings of the International Conference, Montpellier, France, edited by S. Narison [Nucl. Phys. B (Proc. Suppl.) **39B** (1995)]; P. S. Wells, presented at the 22nd SLAC Summer Institute on Particle Physics, Astrophysics and Cosmology, Stanford, California, 1994 (unpublished).
- [2] For recent publications, see, e.g., OPAL Collaboration, R. Akers *et al.*, *Z. Phys. C* **60**, 199 (1993); SLD Collaboration, K. Abe *et al.*, *Phys. Rev. Lett.* **72**, 3145 (1994); OPAL Collaboration, R. Akers *et al.*, *Z. Phys. C* **61**, 209 (1994); A. De Angelis *et al.*, DELPHI Report No. DELPHI 94-94, PHYS 411 (unpublished); ALEPH Collaboration, D. Buskulic *et al.*, *Z. Phys. C* **62**, 1 (1994); **62**, 179 (1994).
- [3] Yu. L. Dokshitzer, V. S. Fadin, and V. A. Khoze, *Phys. Lett.* **115B**, 242 (1982); *Z. Phys. C* **15**, 325 (1982).
- [4] Yu. L. Dokshitzer, V. A. Khoze, and S. I. Troyan, in *Physics in Collision VI*, Proceedings of the Sixth International Conference, Chicago, Illinois, 1986, edited by M. Derrick (World Scientific, Singapore, 1987), p. 417.
- [5] Yu. L. Dokshitzer, in *Physics up to 200 TeV*, Proceedings of the International School of Subnuclear Physics, Erice, Italy, 1990, edited by A. Zichichi, Subnuclear Series Vol. 28 (Plenum, New York, 1991).
- [6] Yu. L. Dokshitzer, V. A. Khoze, and S. I. Troyan, *J. Phys. G* **17**, 1481 (1991); **17**, 1602 (1991).
- [7] Yu. L. Dokshitzer, V. A. Khoze, and S. I. Troyan, “Specific Features of Heavy Quark Production. I. Leading quarks,” Lund Report No. LU TP 92-10 (unpublished); Yu. L. Dokshitzer, in *Perturbative QCD and Hadronic Interactions*, Proceedings of the 27th Rencontres de Moriond, Les Arcs, France, 1992, edited by J. Tran Thanh Van (Editions Frontières, Gif-sur-Yvette, 1992), p. 259.
- [8] V. A. Khoze, in *Proceedings of the 26th International Conference on High Energy Physics* [1], Vol. II, p. 1578; Durham Report No. DTP/93/78 (unpublished).
- [9] C. Peterson *et al.*, *Phys. Rev. D* **27**, 105 (1983); for review, see, e.g., M. Bosman *et al.*, in *Z Physics at LEP*, Proceedings of the Workshop, Geneva, Switzerland, 1989, edited by G. Altarelli, R. Kleiss, and C. Verzegnassi (CERN Report No. 89-08, Geneva, 1989), Vol. 1, p. 267; J. H. Kühn and P. M. Zerwas, in *Heavy Flavours*, edited by A. J. Buras and M. Lindner, Advanced Series in Directions in High Energy Physics (World Scientific, Singapore, 1992), p. 434.
- [10] B. Mele and P. Nason, *Phys. Lett. B* **245**, 635 (1990); *Nucl. Phys.* **B361**, 626 (1991).
- [11] Yu. L. Dokshitzer, V. A. Khoze, A. H. Mueller, and S. I. Troyan, in *Basics of Perturbative QCD*, edited by J. Tran Thanh Van (Editions Frontières, Gif-sur-Yvette, France, 1991).
- [12] V. N. Baier and V. A. Khoze, *Sov. Phys. JETP* **21**, 629 (1965); report, NSU, Novosibirsk, 1964 (unpublished).
- [13] V. S. Fadin and V. A. Khoze, *JETP Lett.* **46**, 525 (1987); *Sov. J. Nucl. Phys.* **48**, 309 (1988).
- [14] G. Altarelli, *Phys. Rep.* **81**, 1 (1982).
- [15] Yu. L. Dokshitzer and D. V. Shirkov, *Z. Phys. C* **67**, 449 (1995).
- [16] L. Trentadue, in *Perturbative QCD and Hadronic Interactions* [7], p. 167.

- [17] V. N. Gribov and L. N. Lipatov, *Sov. J. Nucl. Phys.* **15**, 438 (1972); **15**, 675 (1972).
- [18] G. Curci, W. Furmanski, and R. Petronzio, *Nucl. Phys.* **B175**, 27 (1980).
- [19] G. Altarelli, R. K. Ellis, G. Martinelli, and S. Y. Pi, *Nucl. Phys.* **B160**, 301 (1979).
- [20] W. Furmanski and R. Petronzio, *Phys. Lett.* **97B**, 437 (1980); *Z. Phys. C* **11**, 293 (1982); J. Kalinowski, K. Konishi, P. N. Scharbach, and T. R. Taylor, *Nucl. Phys.* **B181**, 253 (1981); E. G. Floratos, C. Kounnas, and R. Lacaze, *ibid.* **B192**, 417 (1981).
- [21] S. Catani, G. Marchesini, and B. R. Webber, *Nucl. Phys.* **B349**, 635 (1991).
- [22] S. J. Brodsky, G. P. Lepage, and P. R. MacKenzie, *Phys. Rev. D* **28**, 228 (1983); for a recent review, see S. J. Brodsky and H. J. Lu, presented at the Tennessee International Symposium on Radiative Corrections: Status and Outlook, Gatlinburg, Tennessee, hep-ph/9409462, 1994, (unpublished); *Phys. Rev. D* **48**, 3310 (1993).
- [23] F. E. Low, *Phys. Rev.* **110**, 974 (1958); T. H. Burnett and N. M. Kroll, *Phys. Rev. Lett.* **20**, 86 (1968).
- [24] Yu. L. Dokshitzer, V. A. Khoze, and W. J. Stirling, *Nucl. Phys.* **B428**, 3 (1994).
- [25] Ya. I. Azimov, L. L. Frankfurt, and V. A. Khoze, Report No. LNPI-222, 1976 (unpublished); in Proceedings of the XVIII International Conference on High Energy Physics, Tbilisi, 1976, Dubna (unpublished); J. Bjorken, *Phys. Rev. D* **17**, 171 (1978); M. Suzuki, *Phys. Lett.* **71B**, 139 (1977).
- [26] R. L. Jaffe and L. Randall, *Nucl. Phys.* **B412**, 79 (1994).
- [27] Yu. L. Dokshitzer, V. A. Khoze, and S. I. Troyan, "Specific Features of Heavy Quark Production. II. LPHD Approach to Heavy Particle Spectra," Lund Report No. LU TP 94-23 (unpublished).
- [28] V. N. Gribov, "Possible Solution of the Problem of Quark Confinement," Report No. LU TP 91-7, 1991 (unpublished).
- [29] M. B. Voloshin and Yu. M. Zaitsev, *Sov. Phys. Usp.* **30**, 553 (1987).
- [30] I. I. Bigi, M. A. Shifman, N. G. Uraltsev, and A. I. Vainshtein, *Phys. Rev. D* **50**, 2234 (1994); M. Beneke and V. M. Braun, *Nucl. Phys.* **B426**, 301 (1994).
- [31] M. H. Seymour, *Z. Phys. C* **63**, 99 (1994).
- [32] OPAL Collaboration, R. Akers *et al.*, *Z. Phys. C* **67**, 27 (1995); *Phys. Lett. B* **353**, 595 (1995).
- [33] Yu. L. Dokshitzer and B. R. Webber, *Phys. Lett. B* **352**, 451 (1995).
- [34] G. Colangelo and P. Nason, *Phys. Lett. B* **285**, 167 (1992).
- [35] J. Kodaira and L. Trentadue, *Phys. Lett.* **112B**, 66 (1982); C. T. H. Davies, J. Stirling, and B. R. Webber, *Nucl. Phys.* **B256**, 413 (1985); J. C. Collins, D. E. Soper, and G. Sterman, *ibid.* **B250**, 199 (1985); S. Catani, E. d'Emilio, and L. Trentadue, *Phys. Lett. B* **211**, 335 (1988).
- [36] G. Sterman, *Nucl. Phys.* **B281**, 310 (1987); S. Catani and L. Trentadue, *Phys. Lett. B* **217**, 539 (1989); *Nucl. Phys.* **B327**, 323 (1989); **B353**, 183 (1991).
- [37] J. Kodaira and L. Trentadue, *Phys. Lett.* **123B**, 335 (1982); Report No. SLAC-PUB-2934, 1982 (unpublished).
- [38] S. Catani, G. Turnock, B. R. Webber, and L. Trentadue, *Phys. Lett. B* **263**, 491 (1991).
- [39] S. Catani, G. Turnock, and B. R. Webber, *Phys. Lett. B* **272**, 368 (1991).
- [40] Yu. L. Dokshitzer, D. I. Dyakonov, and S. I. Troyan, *Phys. Lett.* **84B**, 234 (1979); *Phys. Rep. C* **58**, 270 (1980); A. Bassetto, M. Ciafaloni, and G. Marchesini, *Nucl. Phys.* **B163**, 477 (1980); G. Curci and M. Greco, *Phys. Lett.* **92B**, 175 (1980).
- [41] G., Parisi and R. Petronzio, *Nucl. Phys.* **B154**, 427 (1979); B. R. Webber and P. Rakow, *ibid.* **B187**, 254 (1981).
- [42] J. Chyla, A. Kataev, and S. A. Larin, *Phys. Lett. B* **267**, 269 (1991).
- [43] A. C. Mattingly and P. M. Stevenson, *Phys. Rev. Lett.* **69**, 1320 (1992).
- [44] P. M. Stevenson, *Phys. Rev. D* **23**, 2916 (1981).
- [45] V. N. Baier, V. S. Fadin, and V. A. Khoze, *Nucl. Phys.* **B65**, 381 (1973).
- [46] J. Schwinger, *Proc. Natl. Acad. Sci. USA* **71**, 5047 (1974).
- [47] Yu. L. Dokshitzer, talk given at the HERA Workshop, DESY, 1993 (unpublished).